

UC Berkeley

UC Berkeley Electronic Theses and Dissertations

Title

Investigating the role of Ede1, an Eps15 homolog, in Clathrin-mediated endocytosis site initiation and maturation in the budding yeast, *Saccharomyces cerevisiae*

Permalink

<https://escholarship.org/uc/item/5x91c2dt>

Author

Lu, Rebecca

Publication Date

2015

Peer reviewed|Thesis/dissertation

Investigating the role of Ede1, an Eps15 homolog, in Clathrin-mediated endocytosis site
initiation and maturation in the budding yeast, *Saccharomyces cerevisiae*

By

Rebecca Lu

A dissertation submitted in partial satisfaction of the requirements for the degree of

Doctor in Philosophy

in

Molecular and Cell Biology

in the

Graduate Division

of the

University of California, Berkeley

Committee in charge:

Professor David G. Drubin, Chair

Professor Randy W. Schekman

Professor Douglas E. Koshland

Professor Daniel A. Fletcher

Fall 2015

Abstract

Investigating the role of Ede1, an Eps15 homolog, in Clathrin-mediated endocytosis site initiation and maturation in the budding yeast, *Saccharomyces cerevisiae*

By

Rebecca Lu

Doctor of Philosophy in Molecular and Cell Biology

University of California, Berkeley

Professor David G. Drubin, Chair

Clathrin-mediated endocytosis (CME) is the process by which plasma membrane and external material are internalized into the cell. This thesis focuses on Ede1, one of the earliest proteins recruited to endocytic sites, to gain insights into the mechanism of site initiation. In *S. cerevisiae*, approximately 60 proteins arrive at plasma membrane (PM) punctae to build and internalize an endocytic vesicle. This process, which occurs in just 1-2 minutes, can be divided into two phases corresponding to the arrival of the early phase proteins and the arrival of the late phase proteins. While the late phase proteins are responsible for internalizing the budding vesicle, the early phase proteins are required to position the late phase machinery on the plasma membrane. Ede1 is a scaffolding protein involved in site initiation and stabilization during the early phase. Deletion of *EDE1* results in fewer site initiations and defects in the timing of vesicle maturation. Here, I dissect the functions of Ede1 to better understand how different domains contribute to its own localization, as well as endocytic site initiation and maturation. We also identify human Eps15 as an Ede1 functional homolog. When expressed in yeast, human Eps15 is recruited to endocytic sites and supports recruitment of yeast coat proteins to those sites. Future studies in human cells will determine the extent of functional crossover between yeast Ede1 and mammalian Eps15 during endocytosis.

Acknowledgements

First, thanks to David and Georjana for providing a fun and educational lab environment for me to do my research. Thanks to all the Drubin/Barnes lab members for teaching me so many things about science and life in general. Lastly, I'd like to thank my family and especially my partner, Nicholas, for sticking it out with me after so many ups and downs.

Table of contents

Acknowledgements.....	i
Table of contents.....	ii
Table of figures.....	iii
Chapter 1: Introduction to Clathrin-mediated endocytosis.....	1
References.....	11
Chapter 2: Ede1 co-localizes with the casein kinase 1, Hrr25.....	16
Materials and methods	22
References.....	25
Chapter 3:.....	27
Materials and methods	47
References.....	51
Chapter 4: Future directions.....	53
References.....	56

List of figures

Figure 1.1 Timeline of Clathrin-mediated endocytosis in budding yeast.....	3
Figure 1.2 Post-translation modifications and activities of endocytic proteins	5
Figure 2.1 Ede1 co-localizes with Hrr25 at endocytic sites.....	20
Figure 2.2 Ede1 co-localizes with Hrr25 over time	21
Figure 2.3 Hrr25 requires Ede1 C-terminal region for endocytic site localization	22
Figure 3.1 Localization of Ede1-GFP truncation mutants	30
Figure 3.2 Ede1-GFP truncation protein expression and lifetimes.....	32
Figure 3.3 A construct containing the coiled-coil domain, third EH domain, and PxxP region is sufficient to recruit coat proteins	34
Figure 3.4 <i>ede1</i> ^{EH3PPCC} Only and <i>ede1</i> ^{ΔCC} internal facilitate endocytic initiation, but not maturation timing.....	37
Figure 3.5 Coiled-coils contribute to endocytic site localization by aggregating Ede1 molecules	40
Figure 3.6 Eps15 can function as an endocytic site initiator in the absence of Ede1	43

Chapter 1: Introduction to Clathrin-mediated endocytosis

Abstract

Clathrin-mediated endocytosis is a robust, essential cellular process that involves the concerted arrival and departure of many different proteins at the plasma membrane. In yeast, live cell imaging has shown that the spatiotemporal dynamics of these proteins is highly stereotyped. Recent work has focused on understanding how the timing and functions of endocytic proteins are regulated. Below I review our current knowledge of the timeline of endocytic site maturation and highlight recent works focusing on how phosphoregulation, ubiquitination, and lipids regulate various aspects of that timeline. This chapter has been submitted as a Cell Science at a Glance article with an accompanying poster (Rebecca Lu, David G. Drubin, Yidi Sun, under review at the *Journal of Cell Science*).

Introduction

Clathrin-mediated endocytosis (CME) is a highly conserved, essential cellular process by which external materials, integral membrane proteins, and membrane phospholipids are internalized into the cell. The process of CME is initially defined by a two-dimensional protein lattice, composed of clathrin and associated coat proteins, which forms a flat sheet on the plasma membrane. As the site matures, the clathrin coat and plasma membrane develop curvature and the membrane invaginates, forming a clathrin-coated pit (CCP). This deep invagination eventually pinches off from the plasma membrane as a clathrin-coated vesicle (CCV). The CCV then un-coats and joins the endosomal system, after which its cargo is either degraded or recycled back to the plasma membrane. CME is especially important for the regulation of ligand-mediated, receptor tyrosine kinase signaling pathways, such as EGFR (epidermal growth factor receptor) and IR (insulin receptor) signaling, wherein CME functions to internalize ligand-bound receptors from the plasma membrane for their routing to the endosomal membrane systems (reviewed in (Di Fiore and Zastrow, 2014; Goh and Sorkin, 2013)). While CME generally maintains cellular homeostasis, it can also be hijacked for entry into cells by certain viruses and bacteria, such as Influenza A and Listeria (McMahon and Boucrot, 2011).

The budding yeast *Saccharomyces cerevisiae* has been an invaluable model organism for studying CME. While clathrin independent internalization pathways in *S. cerevisiae* are under study (Prosser et al., 2011), the major route into the cell is clathrin-mediated, facilitating powerful studies of CME in this organism. Budding yeast are amenable to molecular-genetic manipulations, making it possible to genetically tag proteins of interest with fluorescent proteins for studies on their localization and dynamics at endogenous levels. They are also advantageous for real time imaging because their cells are spherical and individual CME events can be followed from inception at the cortex to internalization into the cytoplasm by viewing from the side using a medial focal plane. Since most CME components are conserved from yeast to humans, principles learned in yeast typically have broad implications. For example, Sla2 is a key protein in yeast CME that links the actin cytoskeleton to the coat machinery. In *sla2Δ* cells, branched actin polymerization is decoupled from the endocytic machinery resulting in an accumulation of actin-tails that stream in from the cortex (Kaksonen et al., 2003). When the human homolog, Hip1R, is knocked down, cells are similarly defective in endocytosis and

accumulate cortical actin structures (Engqvist-Goldstein et al., 2004). It was previously thought that CME in mammalian cells is more complex and irregular than yeast CME, but with the advent of genome editing tools and better ability to identify authentic CME sites, it has been shown that the process is overall very similar in both organisms (Doyon et al., 2011; Hong et al., 2015). While CME has also been well studied in other fungi, such as the fission yeast *Schizosaccharomyces pombe*, we chose to focus on recent highlights from *S. cerevisiae* for the sake of brevity.

In budding yeast, a detailed timeline of the arrival and departure of over 60 proteins at endocytic sites was established in the early-mid 2000's (Merrifield and Kaksonen, 2014). These proteins can be organized into modules by their functions and the timing of their appearance and disappearance at endocytic sites: 1. early proteins, 2. early, middle, and late coat proteins, 3. WASp and Myosin related proteins, 4. actin and actin associated proteins, and 5. scission related proteins (Figure 1.1). While much effort has been put into understanding the spatiotemporal dynamics of these modules with high precision, recent studies have focused on understanding, at a molecular level, what kinds of protein and lipid modifications regulate the progression of events at an individual CME site.

Figure 1.1 Timeline of Clathrin-mediated endocytosis in budding yeast

Cartoon depiction of clathrin mediated endocytosis with an accompanying timeline describing the observed arrival and departure of endocytic proteins at the plasma membrane. The timeline and cartoon are color coordinated, but events in the timeline are not specifically aligned with events depicted in the cartoon. Where actin is more transparent in the cartoon depicts uncertainty in the field regarding the timing of the arrival of actin and the state of membrane curvature at the endocytic site.

Abbreviations used: Clathrin = Clc1, Chc1; AP-2 complex = Apl1, Apl3, Apm4, Aps2; Arp2/3 complex = Arp2, Arp3, Arc15, Arc18, Arc19, Arc35, Arc40; Rvs complex = Rvs161, Rvs167
The cartoon depiction of endocytosis is not drawn to scale.

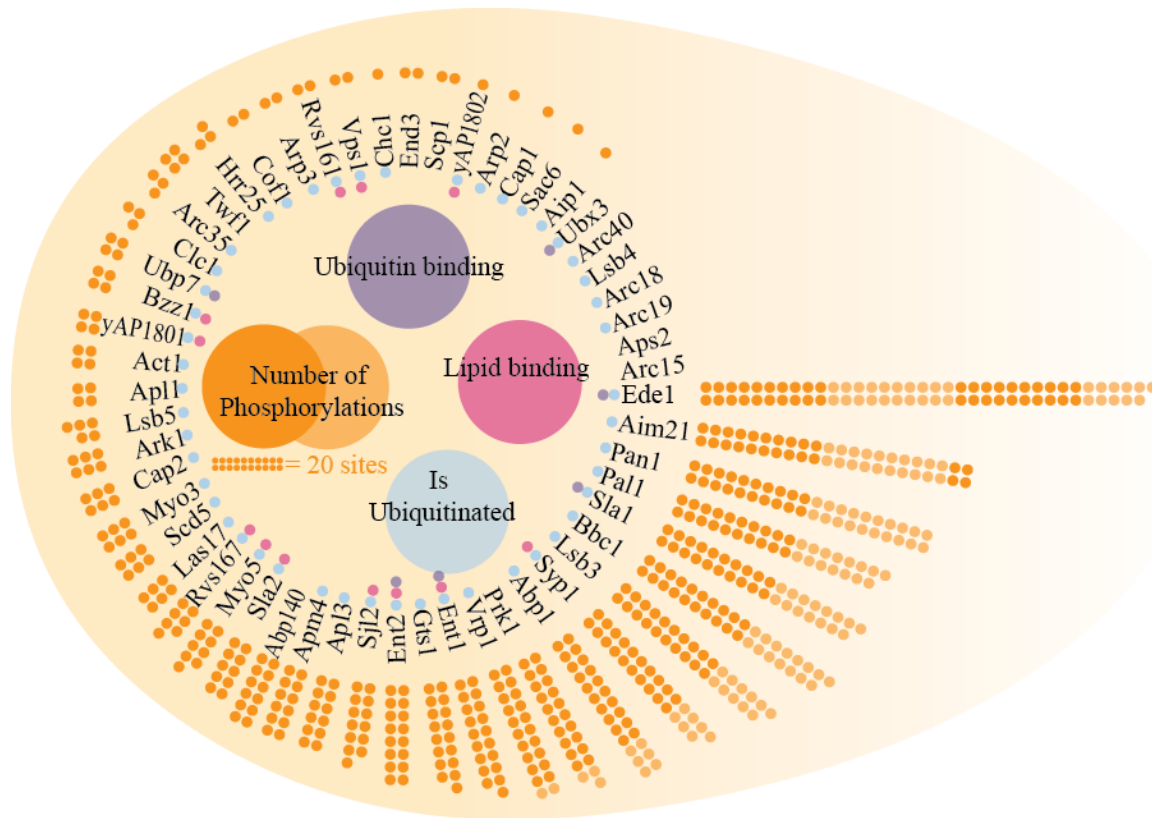


Figure 1.2 Post-translational modifications and activities of endocytic proteins

Dark and light orange circles each indicate one phosphorylation site that has been annotated. Purple dots indicate the protein contains a ubiquitin binding motif or has been shown to bind ubiquitin. Pink dots indicate the protein contains a lipid binding domain or has been shown to bind lipids. Blue dots indicate that the protein has been identified in a ubiquitinated form. The number of phosphorylations and ubiquitinations was annotated from Biogrid (Stark et al., 2010; Stark et al., 2005)

Phosphoregulation

Almost all endocytic proteins across all of the modules are phosphorylated (Figure 1.2). Several kinases and their substrates have been identified at endocytic sites, as well as kinases that have not been found at endocytic sites, but whose activities have effects on endocytosis.

Recently, a member of the conserved casein kinase family, Hrr25, related to CK1 δ/ϵ , was identified as a member of the early protein module and found to phosphorylate the early protein, Ede1 (Figure 1.1, ‘early’ module). A double deletion of both *HRR25* and *EDE1* is synergistic in the reduction of endocytic sites that are formed at the cortex, suggesting a role in endocytic site initiation. In addition to Ede1, Hrr25 also phosphorylates many other proteins across the different modules, such as Sla2, Las17 (WASp), and Aim21 (Peng et al., 2015a). Interestingly, Hrr25 is also involved in many other cellular processes, including autophagy (Tanaka et al., 2014), Golgi trafficking (Lord et al., 2011), DNA damage repair (Hoekstra et al., 1991), and mitotic spindle function (Peng et al., 2015b; Petronczki et al., 2006). Whether Hrr25 coordinates any of these activities with CME needs to be determined.

Several endocytic proteins are also known to be phosphorylated by the Ark kinase family (reviewed in (Smythe and Ayscough, 2003)). Ark1 and Prk1 (Figure 1.1, ‘actin’ module) have well described roles in controlling actin dynamics at endocytic sites and disassembling coat proteins after the CCV has been internalized (Cope et al., 1999; Toret et al., 2008; Zeng and Cai, 1999).

Many endocytic proteins are also substrates of kinases yet to be detected at endocytic sites. Several, such as Abp1, Sla1, and Sla2, are substrates of Cdk1, the master cell cycle regulator (Holt et al., 2009). The type I myosin, Myo5, is regulated by Cka2, which is the catalytic subunit of the holoenzyme CK2 (see ‘lipid requirements and interactions’ below for more details, (Fernández-Golbano et al., 2014)). Hog1 is a stress response MAP kinase that phosphorylates Pan1 and Ede1, which were also found to be hyperphosphorylated during osmotic stress (Reiter et al., 2012). The yeast AGC kinase, Ypk1 and its upstream kinase, Pkh1, are also required for receptor mediated and bulk, fluid phase endocytosis, and are of particular interest because they are also involved in sphingolipid signaling ((Friant et al., 2001; deHart et al., 2002), see ‘lipid functions and interactions’ below). Future studies on these kinase-substrate relationships will determine if and how CME responds to various cellular events and stresses.

To fully understand how phosphoregulation functions in CME, it is also necessary to understand de-phosphorylation. Scd5, a protein phosphatase 1 (PP1, Glc7 in yeast) targeting subunit (Figure 1.1, ‘WASp/Myosin’), counteracts phosphorylation by Ark1 and Prk1 (Chang et al., 2002; Chi et al., 2012; Zeng and Cai, 1999; Zeng et al., 2007). In *scd5* mutants that fail to interact with PP1/Glc7, many endocytic adapter proteins in the coat module are hyperphosphorylated (Chi et al., 2012; Zeng et al., 2007). In addition, lack of Scd5 activity causes a delay in the transition from mid- to late- coat protein progression, likely due to inefficient recruitment of hyperphosphorylated Sla1 (Chi et al., 2012).

Ubiquitination

Ubiquitination of the cytosolic domains of cargo proteins regulates CME internalization in both yeast and mammals (Haglund and Dikic, 2012; Traub and Lukacs, 2007). A long-standing goal is to determine how cargo affects the progression of endocytic site maturation. Ubiquitin likely plays a role in linking cargo to the CME machinery. Three of the known yeast endocytic proteins, Ede1 (UBA, Ubiquitin Associated domain), and Ent1 and Ent2 (UIM, Ubiquitin Interacting Motif), are known to have mono-ubiquitin interacting domains (Figure 1.2). These proteins regulate the ligand-induced internalization of Ste2, the alpha-factor pheromone receptor, which is regulated both by phosphorylation by the casein kinase Yck2 and ubiquitination by the HECT E3 ubiquitin ligase Rsp5 (Dunn and Hicke, 2001a; Dunn and Hicke, 2001b; Toshima et al., 2009). Ent1 and Ede1 are also thought to be recruited to endocytic sites by ubiquitinated cargo (Aguilar et al., 2003).

In addition to conventional ubiquitin interacting domains, one of the SH3 domains of Sla1 also binds ubiquitin (Stamenova et al., 2007). This is intriguing since SH3 domains typically bind to the core peptide motif PxxP, which exists in many endocytic proteins. Interestingly, a PxxP domain bound to this particular ubiquitin binding SH3 domain can be competed off with free ubiquitin (Stamenova et al., 2007). This competition is a potential mechanism for regulating protein-protein interactions in space and time.

Studies have also begun to focus on a role for ubiquitination of the endocytic machinery itself. Many endocytic proteins, including Sla1 and Rvs167, have been identified as targets of Rsp5 (Stamenova et al., 2004). The interaction between the early protein, Ede1, and ubiquitin machinery seems to be particularly important in regulating its functions at the endocytic site. In yeast, deletion of the deubiquitinases, *UBP7* and *UBP2*, whose gene products antagonize Rsp5 mediated ubiquitination, or expression of an Ede1-ubiquitin fusion results in formation of internal punctae, which contain many endocytic proteins and show similar dynamics to *bona fide* CME sites. This result was hypothesized to be due to hyper-ubiquitylated Ede1 and misregulated site initiation. Ubp7 was found to be a component of endocytic sites and shows similar spatiotemporal dynamics to other proteins of the WASp/Myosin module (Figure 1.1, ‘WASp/Myosin’ module) (Weinberg and Drubin, 2014). In addition, a UBX (Ubiquitin Regulatory X) domain containing protein, Ubx3, regulates the rate of Ede1 recruitment to endocytic sites (see ‘late coat’). This regulation by the late arriving Ubx3 is proposed to be mediated by an interaction with Cdc48, a AAA-ATPase ubiquitin-editing complex, but the exact mechanism is still unknown (Farrell et al., 2015). These observations suggest that dynamic ubiquitination and deubiquitination are important for regulating Ede1’s role in CME site initiation and maturation. It will be important to test whether there is a functional relationship between Ede1 ubiquitination and phosphorylation.

Lipid functions and interactions

In almost every module, from early site nucleation to vesicle scission, there is at least one lipid binding protein (Figure 1.2). Lipids are more challenging to study than proteins, yet they nevertheless have very important roles in the endocytic timeline. The lipid-binding activities of endocytic proteins might be important to mediate membrane bending or to harness actin forces.

Turnover of PIP₂ (phosphatidylinositol-4,5-bisphosphate) is required for endocytic function (Sun and Drubin, 2012; Sun et al., 2007). Overproduction of PIP₂ by deleting genes encoding two of the three PIP₂ phosphatases, synaptojanins Sjl1 and Sjl2, leads to a delay in coat and actin disassembly, and defects in fluid phase and receptor-mediated endocytosis, possibly due to a failure in scission (Sun et al., 2007). Sjl2 itself is recruited to endocytic sites (Figure 1.1, ‘scission’ module) by Abp1 (Stefan et al., 2005). Conversely, PIP₂ depletion using a temperature sensitive mutant of the sole budding yeast phosphatidylinositol-4-phosphate-5-kinase, Mss4, results in formation of actin-tails, wherein coat proteins do not internalize, but actin continuously streams inwards from these coat proteins (Sun and Drubin, 2012). The ENTH (Epsin N-terminal homology) and ANTH (AP180 N-terminal homology) PIP₂ binding domains are present in the coat proteins Ent1/2 (intermediate coat), yAP1801/2 (early coat), and Sla2 (intermediate coat) (Aguilar et al., 2003; Carroll et al., 2011; Ford et al., 2001; Itoh et al., 2001; Sun et al., 2004). The ENTH and ANTH domains of Ent1 and Sla2 co-assemble into oligomers in a PIP₂ dependent manner, and are proposed to be responsible for tethering the endocytic machinery to the plasma membrane during membrane tubulation (Skruzny et al., 2012; Skruzny et al., 2015).

Whether and how lipids play a role in site initiation is still an open question. A clue comes from cells in which *RCY1*, whose gene product is involved in endosome-to-Golgi trafficking, is deleted. In *rcy1Δ* cells, PS (phosphatidylserine), but not PIP₂, accumulates on abnormal, internal membrane compartments upon which endocytic proteins accumulate and disappear in the same temporal manner as they do on the plasma membrane, indicating a possible role for PS, specifically, in CME site initiation (Sun and Drubin, 2012). Interestingly, PS is required for cell polarity and is itself localized in a polarized manner, being enriched on the daughter cell (Fairn et al., 2011), where the daughter cell has also been observed to have more endocytic sites than the mother (Bi and Park, 2012). When components in the PS biosynthetic pathway are mutated, endocytic sites also lose their typical polarized localization on the daughter cell (Sun and Drubin, 2012). However, a PS binding protein has yet to be identified specifically at CME sites.

The endocytic role for sphingolipids, including sphingoid bases and ceramides, has been elusive. An *lcb1* mutant, which is deficient in sphingoid base synthesis, the first step in synthesis of more complex sphingolipids, shows a significant defect in internalization of the classic yeast CME cargo, alpha-factor pheromone (Munn and Riezman, 1994; Zanolari et al., 2000). Further studies are needed to understand the mechanism for this phenotype.

Many lipid binding proteins, and specifically proteins that either sense or generate curvature, are involved in the final scission process. The yeast amphiphysin homolog, a heterodimeric complex of Rvs161 and Rvs167, is concentrated along the neck of the growing tubule of a deeply invaginated CCP (Idrissi et al., 2008; Kaksonen et al., 2005; Picco et al., 2015). Bzz1, an F-BAR protein that arrives in the WASP/Myosin module and Rvs161/167 were found to contribute cooperatively to vesicle scission (Kishimoto et al., 2011). Absence of Rvs161/167 results in a “yo-yo” phenotype, wherein coat and cargo components internalize from the cortex, but then retract back to the cortex instead of entering the cell. This phenotype is exacerbated by loss of Bzz1. The lack of Rvs161/167 and Bzz1 results in improper invagination geometry (Kishimoto et al., 2011). Similarly, deletion of *VPS1*, whose gene product is a dynamin-like protein, results in “yo-yo” phenotypes and misshapen invaginations (Rooij et al., 2010), consistent with a role in regulating membrane shape and scission, potentially through an

F-actin bundling activity (Palmer et al., 2015). Unlike other dynamins, Vps1 does not contain a Pleckstrin-homology domain (PH). However, it can still bind and tubulate liposomes (Rooij et al., 2010). While the role of dynamin in scission in yeast CME has been debated, it appears many lipid binding proteins are involved in coordinating the correct geometry of the membrane during endocytosis.

Many studies have focused on how the forces and geometries needed to generate membrane fission can be generated by actin and the late arriving scission proteins. Nevertheless, whether the membrane bends before or after actin arrives appears to be unsettled (Figure 1.1, (Idrissi et al., 2012; Kukulski et al., 2012)). Therefore, determining the geometry of the endocytic membrane and actin network at each stage is an important goal. In yeast, the two type I myosins, Myo3 and Myo5, have essential lipid binding and motor activities (Lewellyn et al., 2015). Fluorescence microscopy showed that these myosins are restricted to the base of growing pits (Jonsdottir and Li, 2004; Picco et al., 2015). However, immunogold labeling and electron microscopy showed that the myosins can also be found at the tip of invaginating pits (Idrissi et al., 2012). Accurate localization of these myosins is particularly important for understanding how the geometry and orientation of myosin driven actin polymerization and lipid binding contribute to the forces required for membrane bending during invagination. For example, spatially regulated phosphorylation and repression of Myo5 actin polymerization by Cka2 is proposed to concentrate branched actin polymerization specifically at the base of endocytic sites (Fernández-Golbano et al., 2014). Interestingly, Syp1, an early arriving protein (Figure 1.1, ‘early’), is an F-BAR protein that interacts and negatively regulates the much later arriving protein Las17 (WASp), *in vitro* (Boettner et al., 2009) to prevent actin polymerization. How this interaction functions *in vivo* remains an open question.

Tying everything together

While we now know when many CME players appear and disappear and where they are located along the invaginating membrane, understanding how this spatiotemporal regulation is achieved is necessary for understanding the underlying mechanisms for this well conserved process. Based on the intriguing observation that early arriving proteins have highly variable lifetimes compared to the very regular timing of later arriving proteins (late coat and beyond), CME can be considered to occur in two temporal phases, an ‘early phase’ and a ‘late phase’.

Recent studies have begun to investigate the molecular basis for these two-phases and their timing. For example, by eliminating certain ‘early phase’ proteins, it was shown that they are not required for ‘late phase’ machinery recruitment and vesicle budding, but instead control the spatial location of the endocytic site (Brach et al., 2014). Expression of a key ‘early phase’ protein, Edel1, at sites typically devoid of CME, results in the recruitment of downstream ‘late phase’ proteins (Brach et al., 2014). In addition, higher order assembly of most of the late phase proteins can be reconstituted *in vitro* by incubating late-phase Las17 (WASp)-coated microspheres in yeast extracts. In these experiments, Las17 (WASp)-coated microspheres nucleated actin filaments and recruited most of the ‘late phase’ proteins, but interestingly, very few of the ‘early phase’ proteins (Michelot et al., 2010), supporting the conclusion that the early phase is separable from the late phase.

Since cargo molecules arrive after the early and early coat proteins, but before the late coat proteins (Toshima et al., 2006), it has been proposed that the transition from irregular to regular lifetimes of later arriving proteins might be controlled by a cargo checkpoint (Carroll et al., 2011), as has been proposed in mammalian cells (Loerke et al., 2009).

Key findings involving the late coat proteins Pan1, End3, and Sla1 have defined a site initiation phase and an actin polymerization phase (Sun et al., 2015). A *pan1* null strain is extremely sick, but with the use of the auxin-inducible degron system, which acutely depletes proteins via degradation by the proteasome (Eng et al., 2014; Nishimura et al., 2009), Pan1 was found to be required for the transition between early CME events and actin assembly (Bradford et al., 2015). Interestingly, when Pan1 and its interaction partner End3 are simultaneously depleted, the ‘early module’ and ‘early-mid coat module’ proteins are capable of localizing with each other at the actin cortex, but the ‘WASp/Myosin’, ‘scission’, and ‘actin’ modules are spatiotemporally uncoupled from the early proteins (Sun et al., 2015). Recruited at the interface between these two functional phases is the cargo adapter Sla1, which is associated with Pan1 and End3. While Sla1 is not the only CME cargo adapter, it is intriguing that it appears at the junction of these two phases, suggesting a possible role coordinating cargo recruitment with actin assembly and vesicle formation. Future studies are required to elucidate the mechanisms and functions underlying this separation of phases.

Acknowledgements

We thank Michelle Lu for helpful advice on figure design and Ross Pedersen for critical reading of the manuscript. We also thank the National Institutes of Health (NIH) for funding.

References

- Aguilar, R. C., Watson, H. A. and Wendland, B.** (2003). The yeast Epsin Ent1 is recruited to membranes through multiple independent interactions. *J Biol Chem*.
- Bi, E. and Park, H.-O.** (2012). Cell polarization and cytokinesis in budding yeast. *Genetics* **191**, 347–87.
- Boettner, D. R., D'Agostino, J. L., Torres, O. T., Daugherty-Clarke, K., Uygur, A., Reider, A., Wendland, B., Lemmon, S. K. and Goode, B. L.** (2009). The F-BAR protein Syp1 negatively regulates WASp-Arp2/3 complex activity during endocytic patch formation. *Current Biology* **19**, 1979–87.
- Brach, T., Godlee, C., Moeller-Hansen, I., Boeke, D. and Kaksonen, M.** (2014). The initiation of clathrin-mediated endocytosis is mechanistically highly flexible. *Current Biology* **24**, 548–54.
- Bradford, M. K., Whitworth, K. and Wendland, B.** (2015). Pan1 regulates transitions between stages of clathrin-mediated endocytosis. *Mol Biol Cell* **26**, 1371–85.
- Carroll, S. Y., Stimpson, H. E. M., Weinberg, J., Toret, C. P., Sun, Y. and Drubin, D. G.** (2011). Analysis of yeast endocytic site formation and maturation through a regulatory transition point. *Mol Biol Cell* **23**, 657–68.
- Chang, J. S., Henry, K., Wolf, B. L., Geli, M. and Lemmon, S. K.** (2002). Protein phosphatase-1 binding to scd5p is important for regulation of actin organization and endocytosis in yeast. *J Biol Chem* **277**, 48002–8.
- Chi, R. J., Torres, O. T., Segarra, V. A., Lansley, T., Chang, J. S., Newpher, T. M. and Lemmon, S. K.** (2012). Role of Scd5, a protein phosphatase-1 targeting protein, in phosphoregulation of Sla1 during endocytosis. *J Cell Sci* **125**, 4728–39.
- Cope, M. J., Yang, S., Shang, C. and Drubin, D. G.** (1999). Novel protein kinases Ark1p and Prk1p associate with and regulate the cortical actin cytoskeleton in budding yeast. *J Cell Biol* **144**, 1203–18.
- Di Fiore, P. P. and Zastrow, von, M.** (2014). Endocytosis, signaling, and beyond. *Cold Spring Harbor ...*
- Doyon, J. B., Zeitler, B., Cheng, J., Cheng, A. T., Cherone, J. M., Santiago, Y., Lee, A. H., Vo, T. D., Doyon, Y., Miller, J. C., et al.** (2011). Rapid and efficient clathrin-mediated endocytosis revealed in genome-edited mammalian cells. *Nat Cell Biol* **13**, 331–7.
- Dunn, R. and Hicke, L.** (2001a). Domains of the Rsp5 ubiquitin-protein ligase required for receptor-mediated and fluid-phase endocytosis. *Mol Biol Cell* **12**, 421–35.
- Dunn, R. and Hicke, L.** (2001b). Multiple roles for Rsp5p-dependent ubiquitination at the internalization step of endocytosis. *J Biol Chem* **276**, 25974–81.
- Eng, T., Guacci, V. and Koshland, D.** (2014). ROCC, a conserved region in cohesin's Mcd1 subunit, is essential for the proper regulation of the maintenance of cohesion and establishment of condensation. *Mol Biol Cell* **25**, 2351–64.

- Engqvist-Goldstein, A. E. Y., Zhang, C. X., Carreno, S., Barroso, C., Heuser, J. E. and Drubin, D. G.** (2004). RNAi-mediated Hip1R silencing results in stable association between the endocytic machinery and the actin assembly machinery. *Mol Biol Cell* **15**, 1666–79.
- Fairn, G. D., Hermansson, M., Somerharju, P. and Grinstein, S.** (2011). Phosphatidylserine is polarized and required for proper Cdc42 localization and for development of cell polarity. *Nat Cell Biol* **13**, 1424–30.
- Farrell, K. B., Grossman, C. and Di Pietro, S. M.** (2015). New Regulators of Clathrin-Mediated Endocytosis Identified in *Saccharomyces cerevisiae* by Systematic Quantitative Fluorescence Microscopy. *Genetics*.
- Fernández-Golbano, I. M., Idrissi, F.-Z., Giblin, J. P., Grosshans, B. L., Robles, V., Grötsch, H., Del Mar Borrás, M. and Geli, M. I.** (2014). Crosstalk between PI(4,5)P₂ and CK2 modulates actin polymerization during endocytic uptake. *Dev Cell* **30**, 746–58.
- Ford, M. G., Pearse, B. M., Higgins, M. K., Vallis, Y., Owen, D. J., Gibson, A., Hopkins, C. R., Evans, P. R. and McMahon, H. T.** (2001). Simultaneous binding of PtdIns(4,5)P₂ and clathrin by AP180 in the nucleation of clathrin lattices on membranes. *Science* **291**, 1051–5.
- Friant, S., Lombardi, R., Schmelzle, T., Hall, M. N. and Riezman, H.** (2001). Sphingoid base signaling via Pkh kinases is required for endocytosis in yeast. *EMBO J* **20**, 6783–92.
- Goh, L. K. and Sorkin, A.** (2013). Endocytosis of receptor tyrosine kinases. *Cold Spring Harbor perspectives in ...*
- Haglund, K. and Dikic, I.** (2012). The role of ubiquitylation in receptor endocytosis and endosomal sorting. *J Cell Sci* **125**, 265–75.
- Hoekstra, M. F., Liskay, R. M., Ou, A. C., DeMaggio, A. J., Burbee, D. G. and Heffron, F.** (1991). HRR25, a putative protein kinase from budding yeast: association with repair of damaged DNA. *Science* **253**, 1031–4.
- Holt, L. J., Tuch, B. B., Villén, J., Johnson, A. D. and Gygi, S. P.** (2009). Global analysis of Cdk1 substrate phosphorylation sites provides insights into evolution. *Science*.
- Hong, S. H., Cortesio, C. L. and Drubin, D. G.** (2015). Machine-Learning-Based Analysis in Genome-Edited Cells Reveals the Efficiency of Clathrin-Mediated Endocytosis. *Cell Rep* **12**, 2121–30.
- Idrissi, F.-Z., Blasco, A., Espinal, A. and Geli, M. I.** (2012). Ultrastructural dynamics of proteins involved in endocytic budding. *Proc Natl Acad Sci USA* **109**, E2587–94.
- Idrissi, F.-Z., Grötsch, H., Fernández-Golbano, I. M., Presciatto-Baschong, C. and Riezman, H.** (2008). Distinct acto/myosin-I structures associate with endocytic profiles at the plasma membrane. *J Cell Biol* **180**, 1219–32.
- Itoh, T., Koshiba, S., Kigawa, T., Kikuchi, A., Yokoyama, S. and Takenawa, T.** (2001). Role of the ENTH domain in phosphatidylinositol-4,5-bisphosphate binding and endocytosis. *Science* **291**, 1047–51.

- Jonsdottir, G. A. and Li, R.** (2004). Dynamics of yeast Myosin I: evidence for a possible role in scission of endocytic vesicles. *Current Biology* **14**, 1604–9.
- Kaksonen, M., Sun, Y. and Drubin, D. G.** (2003). A pathway for association of receptors, adaptors, and actin during endocytic internalization. *Cell* **115**, 475–87.
- Kaksonen, M., Toret, C. P. and Drubin, D. G.** (2005). A modular design for the clathrin- and actin-mediated endocytosis machinery. *Cell* **123**, 305–20.
- Kishimoto, T., Sun, Y., Buser, C., Liu, J., Michelot, A. and Drubin, D. G.** (2011). Determinants of endocytic membrane geometry, stability, and scission. *Proc Natl Acad Sci USA* **108**, E979–88.
- Kukulski, W., Schorb, M., Kaksonen, M. and Briggs, J. A. G.** (2012). Plasma membrane reshaping during endocytosis is revealed by time-resolved electron tomography. *Cell* **150**, 508–20.
- Lewellyn, E. B., Pedersen, R. T. A., Hong, J., Lu, R., Morrison, H. M. and Drubin, D. G.** (2015). An Engineered Minimal WASP-Myosin Fusion Protein Reveals Essential Functions for Endocytosis. *Dev Cell* **35**, 281–94.
- Loerke, D., Mettlen, M., Yarar, D., Jaqaman, K., Jaqaman, H., Danuser, G. and Schmid, S. L.** (2009). Cargo and dynamin regulate clathrin-coated pit maturation. *PLoS Biol* **7**, e57.
- Lord, C., Bhandari, D., Menon, S., Ghassemian, M., Nycz, D., Hay, J., Ghosh, P. and Ferro-Novick, S.** (2011). Sequential interactions with Sec23 control the direction of vesicle traffic. *Nature* **473**, 181–6.
- McMahon, H. T. and Boucrot, E.** (2011). Molecular mechanism and physiological functions of clathrin-mediated endocytosis. *Nature reviews Molecular cell biology*.
- Merrifield, C. J. and Kaksonen, M.** (2014). Endocytic accessory factors and regulation of clathrin-mediated endocytosis. *Cold Spring Harb Perspect Biol* **6**, a016733.
- Michelot, A., Costanzo, M., Sarkeshik, A., Boone, C., Yates, J. R. and Drubin, D. G.** (2010). Reconstitution and protein composition analysis of endocytic actin patches. *Current Biology* **20**, 1890–9.
- Munn, A. L. and Riezman, H.** (1994). Endocytosis is required for the growth of vacuolar H(+)-ATPase-defective yeast: identification of six new END genes. *J Cell Biol* **127**, 373–86.
- Nishimura, K., Fukagawa, T., Takisawa, H., Kakimoto, T. and Kanemaki, M.** (2009). An auxin-based degron system for the rapid depletion of proteins in nonplant cells. *Nat Methods* **6**, 917–22.
- Palmer, S. E., Rooij, I. I. S.-D., Marklew, C. J., Allwood, E. G., Mishra, R., Johnson, S., Goldberg, M. W. and Ayscough, K. R.** (2015). A dynamin-actin interaction is required for vesicle scission during endocytosis in yeast. *Current Biology* **25**, 868–78.

- Peng, Y., Grassart, A., Lu, R., Wong, C. C. L., Yates, J., Barnes, G. and Drubin, D. G.** (2015a). Casein kinase 1 promotes initiation of clathrin-mediated endocytosis. *Dev Cell* **32**, 231–40.
- Peng, Y., Moritz, M., Han, X., Giddings, T. H., Lyon, A., Kollman, J., Winey, M., Yates, J., Agard, D. A., Drubin, D. G., et al.** (2015b). Interaction of CK1 δ with γ TuSC ensures proper microtubule assembly and spindle positioning. *Mol Biol Cell* **26**, 2505–18.
- Petronczki, M., Matos, J., Mori, S., Gregan, J., Bogdanova, A., Schwickart, M., Mechtler, K., Shirahige, K., Zachariae, W. and Nasmyth, K.** (2006). Monopolar attachment of sister kinetochores at meiosis I requires casein kinase 1. *Cell* **126**, 1049–64.
- Picco, A., Mund, M., Ries, J., Nédélec, F. and Kaksonen, M.** (2015). Visualizing the functional architecture of the endocytic machinery. *Elife* **4**.
- Prosser, D. C., Drivas, T. G., Maldonado-Báez, L. and Wendland, B.** (2011). Existence of a novel clathrin-independent endocytic pathway in yeast that depends on Rho1 and formin. *J Cell Biol* **195**, 657–71.
- Reiter, W., Anrather, D., Dohnal, I., Pichler, P., Veis, J., Grötli, M., Posas, F. and Ammerer, G.** (2012). Validation of regulated protein phosphorylation events in yeast by quantitative mass spectrometry analysis of purified proteins. *Proteomics* **12**, 3030–43.
- Rooij, I. I. S.-D., Allwood, E. G., Aghamohammadzadeh, S., Hetteema, E. H., Goldberg, M. W. and Ayscough, K. R.** (2010). A role for the dynamin-like protein Vps1 during endocytosis in yeast. *J Cell Sci* **123**, 3496–506.
- Skruczny, M., Brach, T., Ciuffa, R., Rybina, S., Wachsmuth, M. and Kaksonen, M.** (2012). Molecular basis for coupling the plasma membrane to the actin cytoskeleton during clathrin-mediated endocytosis. *Proc Natl Acad Sci USA* **109**, E2533–42.
- Skruczny, M., Desfosses, A., Prinz, S., Dodonova, S. O., Gieras, A., Uetrecht, C., Jakobi, A. J., Abella, M., Hagen, W. J. H., Schulz, J., et al.** (2015). An organized co-assembly of clathrin adaptors is essential for endocytosis. *Dev Cell* **33**, 150–62.
- Smythe, E. and Ayscough, K. R.** (2003). The Ark1/Prk1 family of protein kinases. Regulators of endocytosis and the actin skeleton. *EMBO Rep* **4**, 246–51.
- Stamenova, S. D., Dunn, R., Adler, A. S. and Hicke, L.** (2004). The Rsp5 ubiquitin ligase binds to and ubiquitinates members of the yeast CIN85-endophilin complex, Sla1-Rvs167. *J Biol Chem*.
- Stamenova, S. D., French, M. E., He, Y. and Francis, S. A.** (2007). Ubiquitin binds to and regulates a subset of SH3 domains. *Molecular cell*.
- Stark, C., Breitkreutz, B.-J., Chatr-Aryamontri, A., Boucher, L., Oughtred, R., Livstone, M. S., Nixon, J., Van Auken, K., Wang, X., Shi, X., et al.** (2010). The BioGRID Interaction Database: 2011 update. *Nucleic Acids Res* **39**, D698–704.
- Stark, C., Breitkreutz, B.-J., Reguly, T., Boucher, L., Breitkreutz, A. and Tyers, M.** (2005). BioGRID: a general repository for interaction datasets. *Nucleic Acids Res* **34**, D535–9.

- Stefan, C. J., Padilla, S. M., Audhya, A. and Emr, S. D.** (2005). The phosphoinositide phosphatase Sjl2 is recruited to cortical actin patches in the control of vesicle formation and fission during endocytosis. *Mol Cell Biol* **25**, 2910–23.
- Sun, Y. and Drubin, D. G.** (2012). The functions of anionic phospholipids during clathrin-mediated endocytosis site initiation and vesicle formation. *J Cell Sci* **125**, 6157–65.
- Sun, Y., Carroll, S., Kaksonen, M., Toshima, J. Y. and Drubin, D. G.** (2007). PtdIns(4,5)P₂ turnover is required for multiple stages during clathrin- and actin-dependent endocytic internalization. *J Cell Biol* **177**, 355–67.
- Sun, Y., Kaksonen, M., Madden, D. T., Schekman, R. and Drubin, D. G.** (2004). Interaction of Sla2p's ANTH domain with PtdIns(4,5)P₂ is important for actin-dependent endocytic internalization. *Mol Biol Cell* **16**, 717–30.
- Sun, Y., Leong, N. T., Wong, T. and Drubin, D. G.** (2015). A Pan1/End3/Sla1 complex links Arp2/3-mediated actin assembly to sites of clathrin-mediated endocytosis. *Mol Biol Cell* **26**, 3841–56.
- Tanaka, C., Tan, L.-J., Mochida, K., Kirisako, H., Koizumi, M., Asai, E., Sakoh-Nakatogawa, M., Ohsumi, Y. and Nakatogawa, H.** (2014). Hrr25 triggers selective autophagy-related pathways by phosphorylating receptor proteins. *J Cell Biol* **207**, 91–105.
- Toret, C. P., Lee, L., Sekiya-Kawasaki, M. and Drubin, D. G.** (2008). Multiple pathways regulate endocytic coat disassembly in *Saccharomyces cerevisiae* for optimal downstream trafficking. *Traffic* **9**, 848–59.
- Toshima, J. Y., Nakanishi, J.-I., Mizuno, K., Toshima, J. and Drubin, D. G.** (2009). Requirements for recruitment of a G protein-coupled receptor to clathrin-coated pits in budding yeast. *Mol Biol Cell* **20**, 5039–50.
- Toshima, J. Y., Toshima, J., Kaksonen, M., Martin, A. C., King, D. S. and Drubin, D. G.** (2006). Spatial dynamics of receptor-mediated endocytic trafficking in budding yeast revealed by using fluorescent alpha-factor derivatives. *Proc Natl Acad Sci USA* **103**, 5793–8.
- Traub, L. M. and Lukacs, G. L.** (2007). Decoding ubiquitin sorting signals for clathrin-dependent endocytosis by CLASPs. *J Cell Sci* **120**, 543–53.
- Weinberg, J. S. and Drubin, D. G.** (2014). Regulation of clathrin-mediated endocytosis by dynamic ubiquitination and deubiquitination. *Current Biology*.
- Zanolari, B., Friant, S., Funato, K., Sütterlin, C., Stevenson, B. J. and Riezman, H.** (2000). Sphingoid base synthesis requirement for endocytosis in *Saccharomyces cerevisiae*. *EMBO J* **19**, 2824–33.
- Zeng, G. and Cai, M.** (1999). Regulation of the actin cytoskeleton organization in yeast by a novel serine/threonine kinase Prk1p. *J Cell Biol* **144**, 71–82.
- Zeng, G., Huang, B., Neo, S. P., Wang, J. and Cai, M.** (2007). Scd5p mediates phosphoregulation of actin and endocytosis by the type 1 phosphatase Glc7p in yeast. *Mol Biol Cell* **18**, 4885–98.

deHart, A. K. A., Schnell, J. D., Allen, D. A. and Hicke, L. (2002). The conserved Pkh-Ypk kinase cascade is required for endocytosis in yeast. *J Cell Biol* **156**, 241–8.

Chapter 2: Ede1 co-localizes with the casein kinase 1, Hrr25

Portions of this chapter represent work that I did in collaboration with Dr. Connie Peng and appear in the publication, “*Casein kinase 1 promotes initiation of clathrin-mediated endocytosis*” (Peng, Y. et al, *Developmental Cell*, 32:2, 231-240).

Introduction

Ede1 is an important endocytic scaffolding protein that is one of the first proteins to arrive at the nascent endocytic site or patch (Reider et al., 2009; Stimpson et al., 2009). Ede1 has roles in endocytic site initiation and maturation (Brach et al., 2014; Carroll et al., 2011). However, our knowledge of the mechanistic details behind these roles is limited. To our best and current knowledge, Ede1 is also the most highly phosphorylated protein that arrives at the endocytic site (Sadowski et al., 2013; Stark et al., 2010). Seventy-one phosphorylation sites have been identified on Ede1 (Sadowski et al., 2013; Stark et al., 2010). Prk1 kinase phosphorylates Ede1 (Mok et al., 2010), but these phosphorylations are likely to regulate endocytic disassembly since Prk1 arrives at the endocytic site when the vesicle is about to internalize (Toret et al., 2008). We sought to identify other kinases that phosphorylate Ede1 and asked if they might be involved in Ede1 regulation.

Results

Ede1 was identified as a substrate of the casein kinase I, Hrr25 (Breitkreutz et al., 2010; Ho et al., 2002; Peng et al., 2015). To test whether Hrr25 is recruited to endocytic sites and its relation to Ede1, we generated a strain containing Hrr25 tagged at the C-terminus with three repeats of green fluorescent protein (3xGFP) and Ede1 tagged at the C-terminus with red fluorescent protein (RFP). Using simultaneous dual-color imaging, we analyzed still images by eye and found that Hrr25 co-localizes with Ede1 in 77% of the patches counted (Figure 2.1 A,C). This is comparable to colocalization with a well-known Ede1 binding partner, Syp1, which is also known to be recruited to patches with Ede1 (Carroll et al., 2011; Stimpson et al., 2009). Ede1 co-localizes with Syp1 in 78% of the patches counted (Figure 2.1 B, C). Since Hrr25 co-localized with Ede1 in the vast majority of patches in still images, we concluded that it was very likely that, similar to Syp1, Hrr25 has similar temporal dynamics to Ede1 at endocytic sites.

Knowing this, we wanted to further test whether Hrr25 arrived before or after Ede1. To accomplish this, we attempted to image the same strain described above (*EDE1-RFP, HRR25-3xGFP*) using simultaneous dual color, time-lapse imaging. However, we found that RFP had low signal-to-noise and photo-bleached rapidly under our imaging conditions. To overcome this obstacle, we chose to tag Ede1 with mCherry, another monomeric red fluorescent protein that is known to be more photostable than RFP (Shaner et al., 2004). Although Ede1-mCherry is brighter and more photostable than Ede1-RFP, Hrr25-3xGFP also shows low signal-to-noise ratio either because of high cytosolic background or low molecule numbers at endocytic sites. To maximize the signal received by the camera, we used imaging conditions with relatively low time resolution (one frame every four seconds) to minimize bleaching in the green channel and a 60x objective, which lowers spatial resolution, but also gathers more light than a 100x objective (see materials and methods). Using this strain expressing Ede1-mCherry and Hrr25-3xGFP, we performed live cell imaging over four minutes. Using kymograph analysis, we found that Ede1

and Hrr25 generally co-localize for at least a portion of their lifetimes. In these movies, 66% of the patches analyzed contained both Ede1 and Hrr25 at some point during their lifetime at the plasma membrane (Figure 2.2 A,C). This level of co-localization is, again, similar to that observed for Ede1-mCherry and Syp1-GFP when imaged under the same conditions (74%, Figure 2.2 B,C). With this time resolution, we also found that Hrr25 did not consistently arrive before or after Ede1 (Figure 2.2 D, E). Instead, we see Hrr25 arriving with Ede1 20% of the time. Hrr25 arrives before Ede1 31% of the time, and arrives after Ede1 49% of the time, typically within 40 seconds on each side. From these results, we conclude that Hrr25 arrives at endocytic sites at approximately the same time as Ede1. The fact that Hrr25 does not arrive consistently before or after Ede1 is similar to results found for other early arriving proteins (Carroll et al., 2011).

Because other early proteins (Syp1, clathrin, Pal1, yAP1801, AP-2 complex) are known to rely on Ede1 for proper localization to endocytic sites (Carroll et al., 2011), we also tested whether Hrr25 depends on Ede1 for localization. We found that deletion of *EDE1* results in loss of Hrr25 recruitment to the plasma membrane. However, Hrr25 can still be seen at the yeast spindle pole body, indicating that Ede1 dependent localization is specific for endocytic sites (Peng et al., 2015). We then asked which domains of Ede1 are important for Hrr25 localization to endocytic sites. To address this, we generated strains with C-terminal 13xmyc tagged truncations of Ede1 and Hrr25-3xGFP (Figure 2.3A). Truncation of the UBA (ubiquitin associated) domain did not have an appreciable effect on Hrr25 localization (Figure 2.3B). However, truncation of the amino acids between the coiled-coils and the UBA domain (900-1341) resulted in loss of Hrr25 localization at endocytic sites, but not at spindle pole bodies (Figure 2.3B). Western blot analysis showed that this was not a result of inefficient protein expression (Figure 2.3C). Therefore, the Ede1 C-terminal region is specifically necessary for Hrr25 recruitment to endocytic sites.

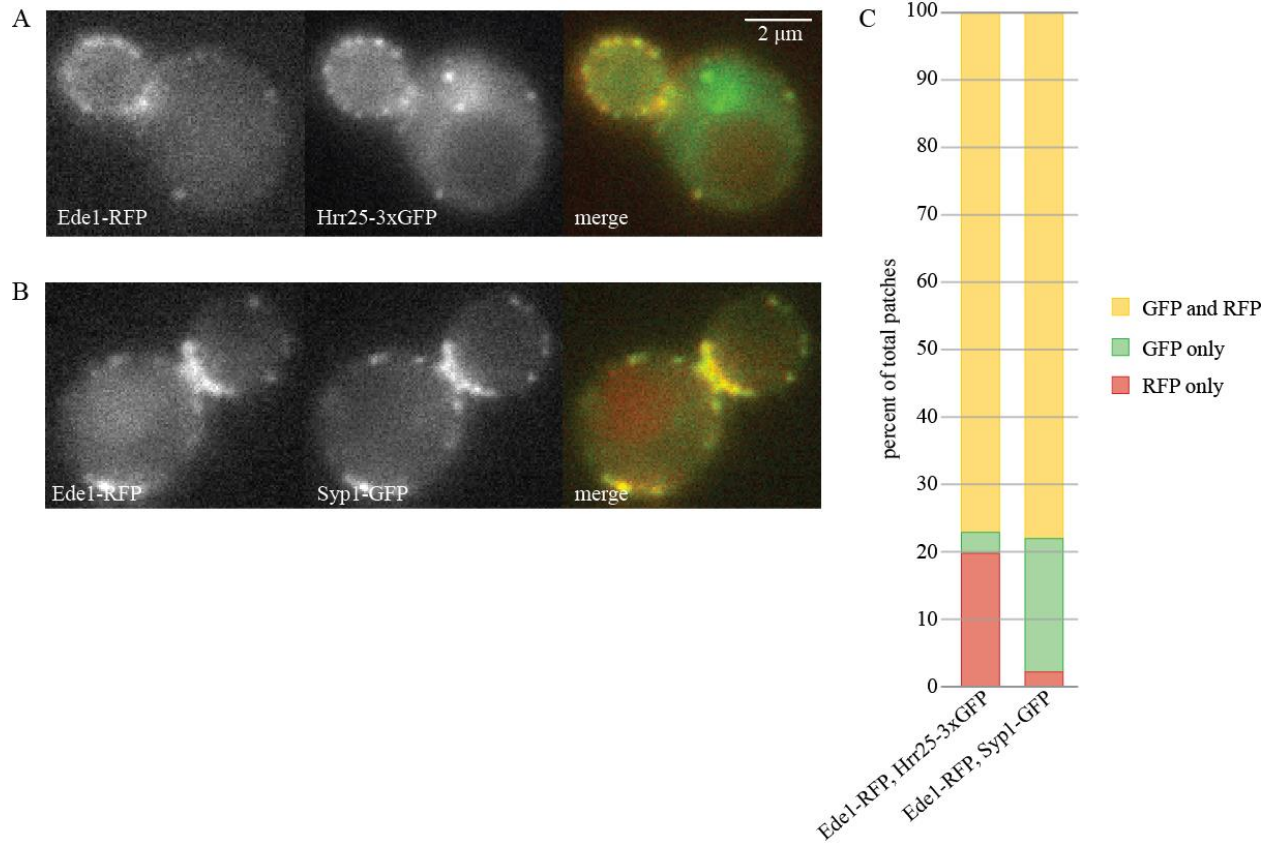
Discussion

CME is a complex process that involves the concerted arrival and departure of over 60 proteins at plasma membrane sites. How these sites are initiated is not well understood. Ede1 is one of the earliest arriving proteins and is thought to have a role in site initiation. To better understand site initiation, we chose to study the mechanisms of Ede1 regulation. It has been shown that Ede1 is a highly phosphorylated protein (Sadowski et al., 2013; Stark et al., 2010) and that the casein kinase Hrr25 phosphorylates Ede1 (Peng et al., 2015).

In this study we focused on the dynamic localization of Ede1 and Hrr25 at endocytic sites. To better understand when Hrr25 might interact with Ede1, and therefore when phosphorylation might take place, we used dual-color live cell imaging to image Ede1 and Hrr25 simultaneously. We found that Ede1 and Hrr25 have similar dynamics and a high degree of co-localization. Also, one does not consistently arrive before the other, which may indicate that Hrr25 may arrive at endocytic sites, but requires Ede1 to stabilize its localization since *ede1Δ* cells lack Hrr25 at endocytic sites. We also mapped the region of Ede1 that is required for Hrr25 endocytic site localization to the C-terminal region of Ede1 between amino acid residues 900 and 1341. Interestingly, this region contains a high density of phosphorylation sites (Sadowski et al.,

2013; Stark et al., 2010) and is specifically phosphorylated by Hrr25 in an *in vitro* kinase assay (Peng et al., 2015).

These results provide groundwork for understanding how phosphorylation regulates endocytosis, and specifically, its role in regulation of endocytic site initiation.



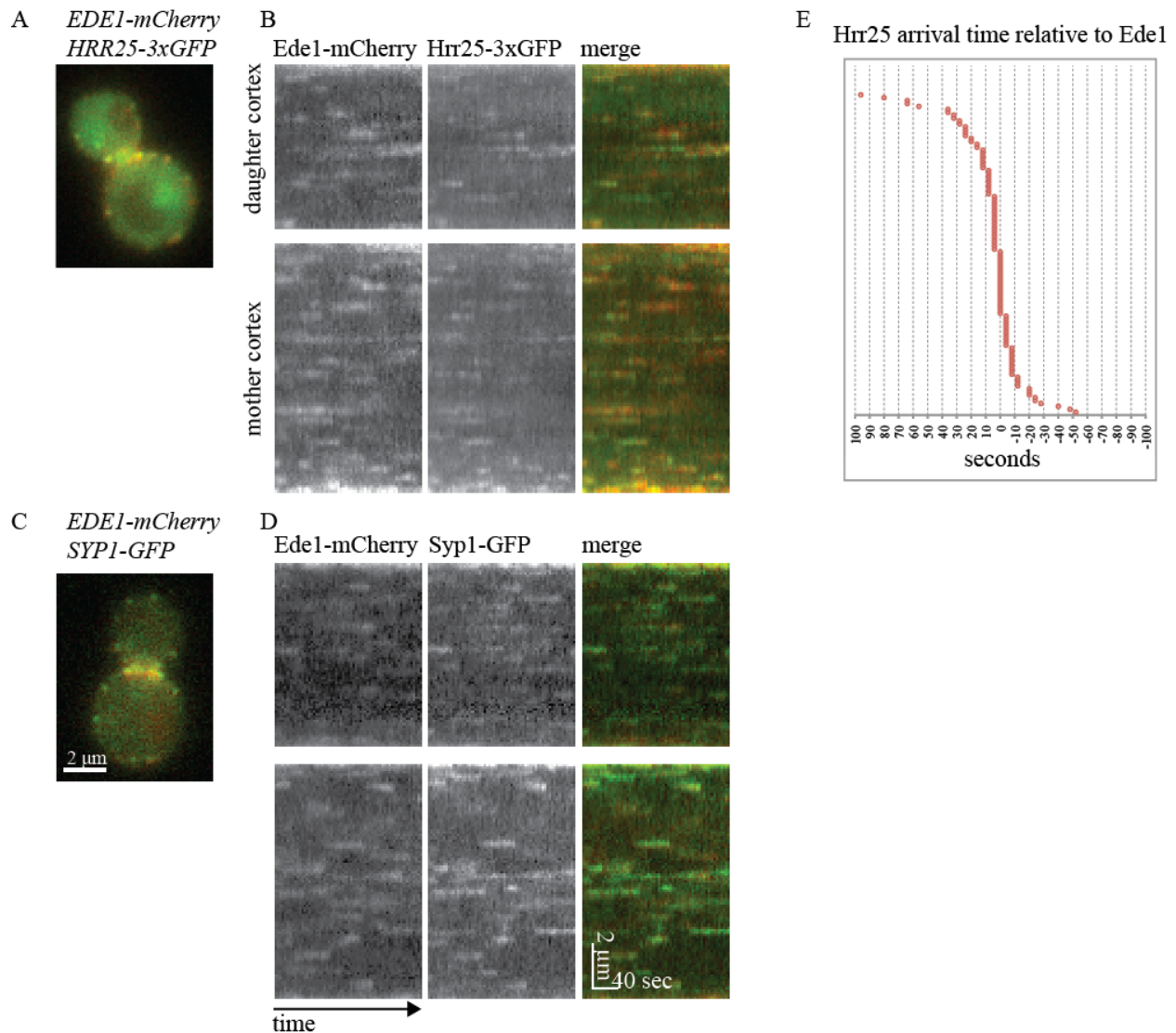


Figure 2.2 Ede1 co-localizes with Hrr25 over time

(A, C) A representative image of a yeast cell expressing Ede1-mCherry and Hrr25-3xGFP (A) or Syp1-GFP (C). (B,D) Kymographs taken from around the daughter cortex (top) and mother cortex (bottom) of the cells shown in (A) and (C). Scale bars 2 μm and 40 sec. (E) Graphical representation of Hrr25 arrival time at individual endocytic sites relative to Ede1 arrival. Each point represents an individual site. (n=23 cells, 110 sites). Negative and positive values indicate arrival time before and after Ede1.

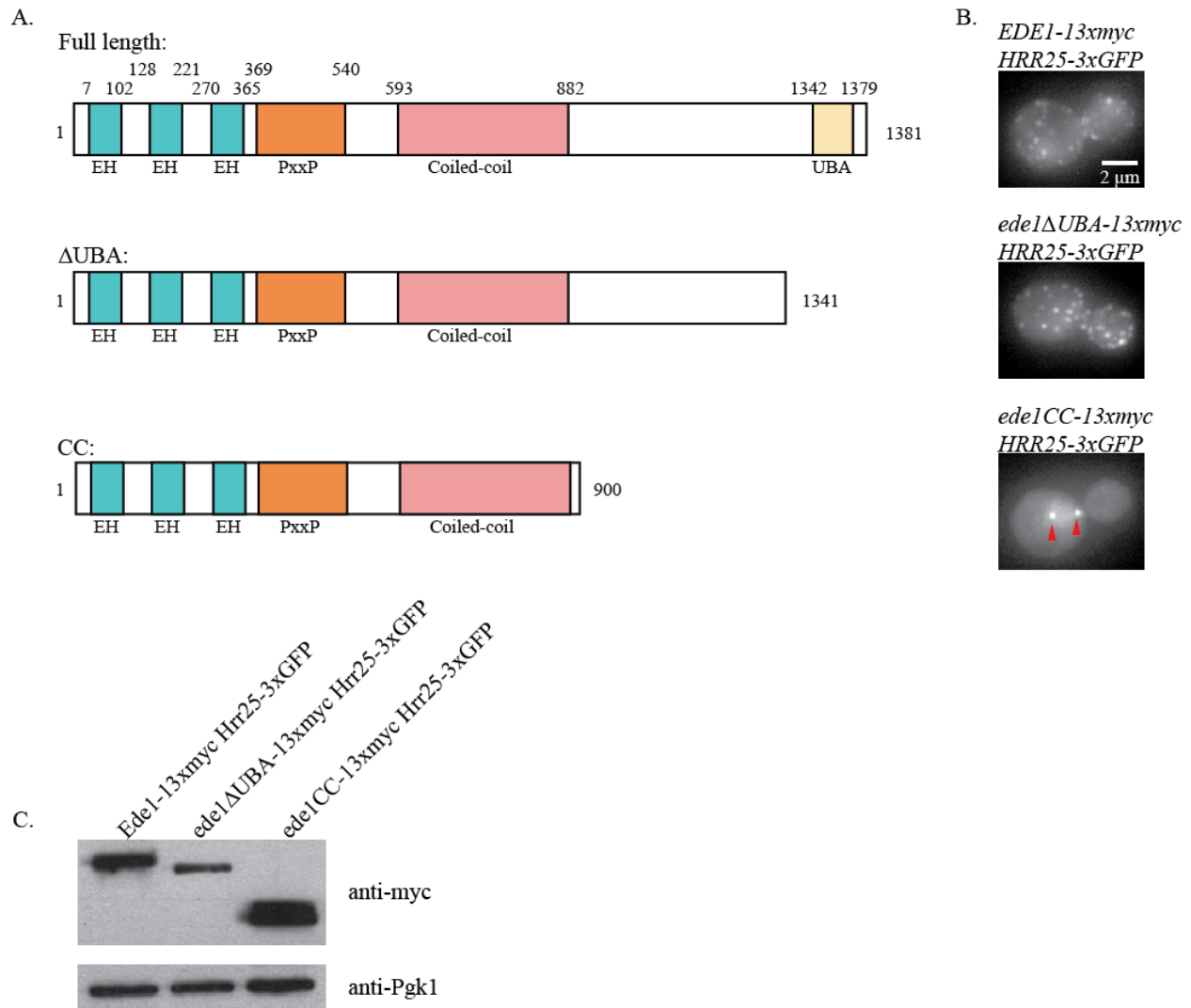


Figure 2.3 Hrr25 requires Ede1 C-terminal region for endocytic site localization

(A) Schematic diagram of full-length Ede1 and the truncation constructs that were integrated at the *EDE1* locus. A C-terminal 13xmyc tag on all constructs is not shown. Numbers indicate amino acid residues. EH, Eps15 homology; PxxP, proline-rich; UBA, ubiquitin associated domain. (B) Representative images of maximum intensity Z-stack projections of cells with the indicated genotype. Red arrowheads in bottom panel indicate spindle pole bodies. Scale bar, 2 μ m. (C) Whole cell extracts of the indicated genotype were analyzed by immunoblot using anti-myc and anti-Pgk1 (loading control) antibodies.

Materials and methods

Yeast strains

Cells were maintained on rich media (YPD) at either 25°C or 30°C.

Strain	Genotype
DDY4370	<i>MATa his3Δ200 leu2-3,112 ura3-52 HRR25-3GFP::HIS3</i>
DDY4372	<i>MATa his3Δ200 leu2-3,112 ura3-52 HRR25-3GFP::HIS3 EDE1-mCherry::KanMX</i>
DDY4591	<i>MATa his3Δ200 leu2-3,112 ura3-52 SYP1-GFP::KanMX EDE1-mCherry::KanMX</i>
DDY4387	<i>MATa his3Δ200 leu2-3,112 ura3-52 HRR25-3GFP::HIS3 EDE1-MYC::HIS3</i>
DDY4390	<i>MATa his3Δ200 leu2-3,112 ura3-52 HRR25-3GFP::HIS3 ede1ΔUBA-MYC::HIS3</i>
DDY4391	<i>MATa his3Δ200 leu2-3,112 ura3-52 HRR25-3GFP::HIS3 ede1CC-MYC::HIS3</i>
CPY1132	<i>MATa his3Δ200 leu2-3,112 ura3-52 HRR25-3GFP::HIS3 EDE1-RFP::HIS</i>
DDY3871	<i>MATα his3Δ200 leu2-3,112 ura3-52 lys2-801 SYP1-GFP::KanMX6 EDE1-RFP::HIS3</i>
DDY1102	<i>MATa/α his3Δ200/ his3Δ200 leu2-3,112/ leu2-3,112 ura3-52/ ura3-52 lys2-801/LYS2</i>

Live imaging and image analysis

Cells were grown to log phase at 25°C in imaging media (synthetic medium lacking tryptophan) and immobilized on concanavalin A-coated coverslips. Images, except those presented in Figure 2.2, were obtained using MetaMorph software (Molecular Devices) and an Olympus IX81 microscope equipped with a 100x NA 1.4 objective and an Orca-ER camera (Hamamatsu). Images presented in Figure 2.2 were obtained using a 60x NA 1.45 objective. Simultaneous two-color imaging was performed on the Olympus IX81 using a 488 nm argon-ion laser (Melles Griot) and a mercury lamp filtered through a 575/20-nm filter. Z-stacks in Figure 2.3 were obtained at 0.4 μm steps for a total of 6 μm and a maximum intensity projection was produced with MetaMorph software.

Images were processed using ImageJ (NIH) as previously described to threshold background noise (Kaksonen et al., 2003). Circular kymographs were generated using the segmented line tool to draw a circle around the cortex of the mother and daughter of a budding cell. Co-localization analysis was performed manually by inspecting both red and green channels.

Immunoblotting

Yeast total cell extracts were prepared from log-phase cells as previously described (Foiani et al., 1994). Total cell extracts were subjected to SDS-PAGE and immunoblot analysis using mouse anti-myc (9E10) and mouse anti-Pgk1 (Invitrogen) antibodies.

References

- Brach, T., Godlee, C., Moeller-Hansen, I., Boeke, D. and Kaksonen, M. (2014). The initiation of clathrin-mediated endocytosis is mechanistically highly flexible. *Current Biology* 24, 548–54.
- Breitkreutz, A., Choi, H., Sharom, J. R., Boucher, L., Neduva, V., Larsen, B., Lin, Z.-Y., Breitkreutz, B.-J., Stark, C., Liu, G., et al. (2010). A global protein kinase and phosphatase interaction network in yeast. *Science* 328, 1043–6.
- Carroll, S. Y., Stimpson, H. E. M., Weinberg, J., Toret, C. P., Sun, Y. and Drubin, D. G. (2011). Analysis of yeast endocytic site formation and maturation through a regulatory transition point. *Mol Biol Cell* 23, 657–68.
- Foiani, M., Marini, F., Gamba, D., Lucchini, G. and Plevani, P. (1994). The B subunit of the DNA polymerase alpha-primase complex in *Saccharomyces cerevisiae* executes an essential function at the initial stage of DNA replication. *Mol Cell Biol* 14, 923–33.
- Ho, Y., Gruhler, A., Heilbut, A., Bader, G. D., Moore, L., Adams, S.-L., Millar, A., Taylor, P., Bennett, K., Boutilier, K., et al. (2002). Systematic identification of protein complexes in *Saccharomyces cerevisiae* by mass spectrometry. *Nature* 415, 180–3.
- Kaksonen, M., Sun, Y. and Drubin, D. G. (2003). A pathway for association of receptors, adaptors, and actin during endocytic internalization. *Cell* 115, 475–87.
- Mok, J., Kim, P. M., Lam, H. Y. K., Piccirillo, S., Zhou, X., Jeschke, G. R., Sheridan, D. L., Parker, S. A., Desai, V., Jwa, M., et al. (2010). Deciphering protein kinase specificity through large-scale analysis of yeast phosphorylation site motifs. *Sci Signal* 3, ra12.
- Peng, Y., Grassart, A., Lu, R., Wong, C. C. L., Yates, J., Barnes, G. and Drubin, D. G. (2015). Casein kinase 1 promotes initiation of clathrin-mediated endocytosis. *Dev Cell* 32, 231–40.
- Reider, A., Barker, S. L., Mishra, S. K., Im, Y. J., Maldonado-Báez, L., Hurley, J. H., Traub, L. M. and Wendland, B. (2009). Syp1 is a conserved endocytic adaptor that contains domains involved in cargo selection and membrane tubulation. *EMBO J* 28, 3103–16.
- Sadowski, I., Breitkreutz, B.-J., Stark, C., Su, T.-C., Dahabieh, M., Raithatha, S., Bernhard, W., Oughtred, R., Dolinski, K., Barreto, K., et al. (2013). The PhosphoGRID *Saccharomyces cerevisiae* protein phosphorylation site database: version 2.0 update. *Database (Oxford)* 2013, bat026.
- Shaner, N. C., Campbell, R. E., Steinbach, P. A., Giepmans, B. N. G., Palmer, A. E. and Tsien, R. Y. (2004). Improved monomeric red, orange and yellow fluorescent proteins derived from *Discosoma* sp. red fluorescent protein. *Nat Biotechnol* 22, 1567–72.
- Stark, C., Su, T.-C., Breitkreutz, A., Lourenco, P., Dahabieh, M., Breitkreutz, B.-J., Tyers, M. and Sadowski, I. (2010). PhosphoGRID: a database of experimentally verified in vivo protein phosphorylation sites from the budding yeast *Saccharomyces cerevisiae*. *Database (Oxford)* 2010, bap026.

Stimpson, H. E. M., Toret, C. P., Cheng, A. T., Pauly, B. S. and Drubin, D. G. (2009). Early-arriving Syp1p and Ede1p function in endocytic site placement and formation in budding yeast. *Mol Biol Cell* 20, 4640–51.

Toret, C. P., Lee, L., Sekiya-Kawasaki, M. and Drubin, D. G. (2008). Multiple pathways regulate endocytic coat disassembly in *Saccharomyces cerevisiae* for optimal downstream trafficking. *Traffic* 9, 848–59.

Chapter 3: Selection and stabilization of endocytic sites by Ede1, a yeast functional homolog of the human Eps15

Introduction

As previously mentioned, the mechanisms behind endocytic site initiation and maturation in *S. cerevisiae* are not well understood. Gaining a better understanding of these mechanisms will provide insight into other questions, such as a possible role for cargo capture and how and whether other events in the cell, such as cell cycle progression, affect endocytosis.

Of the 60 proteins that are known to arrive at the endocytic site, eight are members of the “early-phase”: Ede1, Syp1, Hrr25, clathrin, AP-2 complex, and Pal1. The duration of time these proteins spend at individual endocytic sites, i.e. their “lifetimes”, can vary widely from tens of seconds to a few minutes (Carroll et al., 2011; Carroll et al., 2009; Newpher et al., 2005; Peng et al., 2015; Stimpson et al., 2009). Early phase proteins play an important role in efficient site initiation, though they are dispensable for endocytic vesicle formation and internalization. Depletion of early phase proteins does not prevent recruitment and internalization of coat proteins and actin (Brach et al., 2014). Ede1 is among the earliest proteins to arrive at a nascent endocytic site and it facilitates CME initiation and maturation. Deletion of *EDE1* impairs endocytosis in multiple ways, including fewer site initiation events (Kaksonen et al., 2005) and a decrease in the lifetimes of many other endocytic proteins (Carroll et al., 2011; Stimpson et al., 2009). Overall, the rate of endocytosis was reported to be reduced by approximately 35% in an *ede1Δ* cell (Gagny et al., 2000). Recently, it was shown that when Ede1 is artificially recruited to Pil1 patches, it is sufficient to specify the localization of downstream endocytic coat and actin proteins (Brach et al., 2014). Although it is clear that Ede1 plays a central role in site initiation and CME function, the mechanisms underlying Ede1 function for site selection at the PM are poorly understood. Given the important and varied roles that Ede1 has in organizing endocytic sites, we systematically dissected it to determine the roles of each of its domains. Through these studies, we aimed to determine the functions of the domains in site selection and maturation.

Ede1 is a large (1381 amino acids), multi-domain protein thought to function as a dual clathrin adapter/scaffolding protein (Maldonado-Báez et al., 2008). Ede1 is also required for the efficient recruitment of other early-phase proteins to endocytic sites (Carroll et al., 2011). In humans, the endocytic protein Eps15 (EGFR pathway substrate clone 15) shares a similar domain architecture to Ede1 (Confalonieri and Di Fiore, 2002; Reider et al., 2009). Similar to Ede1 in yeast, Eps15 is known to arrive at CCPs in the early stages of site initiation along with AP-2 and FCHo1/2 in mammalian cells (Taylor et al., 2011). However, whether Eps15 functions during endocytic site initiation like Ede1 is still unknown.

While Ede1 has been proposed to be a yeast homolog of Eps15, other yeast proteins also have similar domain structures, and they have also been proposed to be Eps15 homologues. For example, the yeast coat protein Pan1 has been previously hypothesized to be the primary Eps15 homolog (Wendland et al., 1996). However, although Pan1 is a large multi-domain protein like Eps15, its arrival and departure at the endocytic site occurs much later than Ede1. Furthermore, unlike Ede1 and Eps15, which do not internalize and instead remain restricted to the rim of growing CCPs (Tebar et al., 1996), Pan1 is internalized with the endocytic pit (Kaksonen et al.,

2003). Finally, Eps15 forms dimers and tetramers, and its oligomerization state is thought to facilitate recruitment of the AP-2 adapter protein complex, and therefore clathrin, to the rim of the growing pit (Cupers et al., 1998; Tebar et al., 1997). Ede1 was recently shown to oligomerize in the yeast cytoplasm through its coiled-coil domain (Boeke et al., 2014). Ede1 mutants that fail to oligomerize cannot recruit a well-known Ede1 binding partner, Syp1, to endocytic sites, similar to *ede1* Δ mutants. Artificial dimerization of the EH domains partially rescued Syp1 plasma membrane recruitment (Boeke et al., 2014). Based on these comparisons, we hypothesize that Eps15 is an Ede1 functional homolog and sought to test this possibility by expressing Eps15 in yeast.

Results

The Ede1 coiled coil domain is required but not sufficient for punctate, plasma membrane localization

The architecture of Ede1 is defined by several domains and motifs. Ede1 is characterized by its three N-terminal Eps15-homology (EH) domains that are predicted to bind to the Asn-Pro-Phe tri-peptide motif (Confalonieri and Di Fiore, 2002; Miliaras and Wendland, 2004) (Figure 3.1A, full length). These are followed by proline (PxxP) rich and central coiled-coil (CC) domains (Reider et al., 2009). The Ede1 C-terminus is defined by a ubiquitin-associated domain (UBA). Between the coiled-coils and the UBA domain is a largely unstructured region that is highly phosphorylated by the casein kinase Hrr25 (Peng et al., 2015).

To better understand the functions of Ede1's domains, we generated multiple truncations of EDE1 and integrated these into the endogenous locus fused to a C-terminal green fluorescent protein (GFP) tag (Figure 3.1A). We initially set out to determine which domains of Ede1 contribute to endocytic site localization. We compared the expression of the truncation constructs by imaging the truncation strains in the same field of view as strains expressing full-length Ede1-GFP. Ede1-GFP strains were distinguished from the Ede1 truncation strains by the use of the lipophilic dye FM4-64, which is internalized to the vacuole (Figure 3.1B). Ede1-GFP kymographs show many punctate patches that are clearly distinguishable from background, and which appear and disappear with variable lifetimes while truncations lacking the coiled-coil domain were poorly recruited to the PM as seen in circular kymographs drawn around the cell cortex (Figure 3.1B-E). Indeed, consistent with previous studies (Boeke et al., 2014) in which only the coiled-coil domains were deleted, we found that every construct missing the coiled-coil domain (PP-, EH3-, and Δ CC_{internal}-GFP) resulted in kymographs showed fewer, dimmer patches. Additionally, we found that deletion of the UBA domain and a highly phosphorylated C-terminal region between amino acids 900-1341 (Peng et al., 2015), or deletion of the PxxP region, did not have any effect on Ede1 localization or lifetime (Figure 3.1B-E, Figure 3.2B *ede1*CC-GFP, *ede1* Δ PP_{internal}-GFP). Based on our analysis of this panel of truncations, we conclude that the coiled-coil domain contributes the most of any Ede1 domain to PM localization (Figure 1B-E, *ede1*CC-GFP vs *ede1*PP-GFP still images and kymographs).

While our findings are largely consistent with those made in previous studies, contrary to Boeke, et al, we found that expression of the coiled-coil domain alone was not sufficient for PM localization (Figure 3.1B-E, CC_{only}-GFP). A possible explanation for this incongruence is that

protein expression levels of CConly-GFP are significantly lower than for Ede1-GFP (Figure 3.2A), which may contribute to its lack of PM localization. However, a truncation containing the coiled-coil domain, the PxxP rich region, and the third EH domain (Figure 3.1B-E, EH3PPCConly-GFP) was recruited to distinct plasma membrane patches despite low expression relative to Ede1-GFP (Figure 3.2A). This construct also had much shorter lifetimes than full length Ede1-GFP (13.5 ± 11.7 sec 57.2 ± 44.2 sec, s.d.; Figure 3.3A). The recruitment of EH3PPCConly-GFP to plasma membrane punctae is particularly striking as it lacks many of Ede1's protein interaction domains and many of its phosphorylation sites.

Because EH3PPCConly-GFP is present on the plasma membrane, we next sought to determine whether EH3PPCConly-GFP-containing patches could recruit downstream endocytic machinery. Toward this end, we used a strain expressing EH3PPCConly-GFP and Sla1 tagged at the C-terminus with mCherry (Sla1-mCherry). Sla1 is a coat protein that arrives after Ede1, but before actin polymerization and internalization (Goode et al., 2015; Weinberg and Drubin, 2011), making it an ideal reporter for successful recruitment and function of downstream endocytic components. Using time lapse imaging over four minutes, we found that in control cells (Ede1-GFP, Sla1-mCherry) 91% of GFP patches recruited mCherry. In the EH3PPCConly-GFP strain, the majority of GFP patches (83%) recruited Sla1-mCherry, despite the fact that much of the protein is missing (Figure 3.3B, C). However, compared to the strain expressing full length Ede1, more patches that contained Sla1-mCherry alone were observed in the EH3PPCConly-GFP strain (Figure 3.3B, arrows; Figure 3.3C "Sla1-mCherry only" 12.3% vs. 0.8% of total patches). This may be the result of lower EH3PPCConly-GFP expression or may be due to the fact that the protein is missing many of its protein interaction domains, or a combination of these two factors. In addition to Sla1, the coat protein Sla2-mCherry was also recruited to EH3PPCConly-GFP patches (Figure 3.3D).

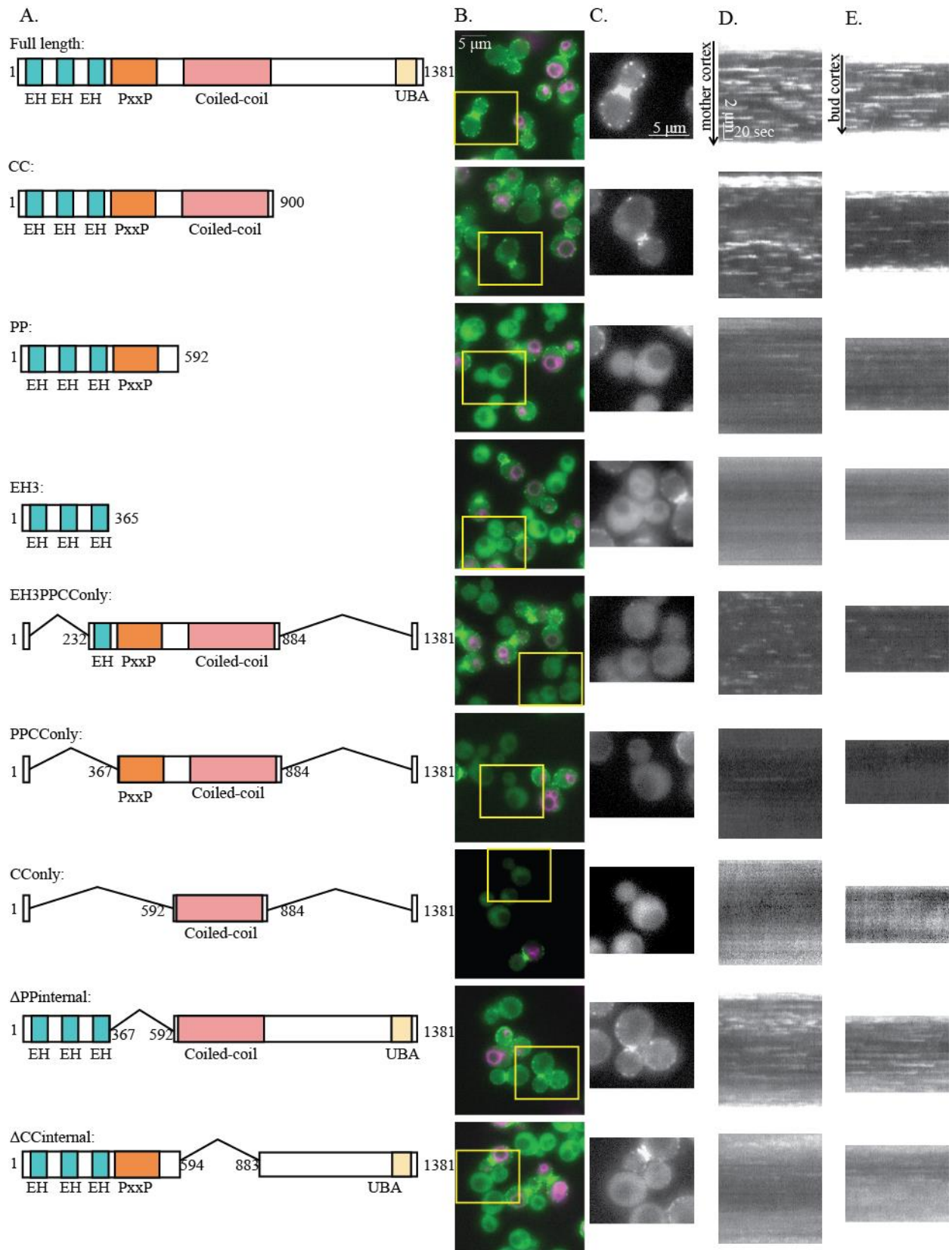
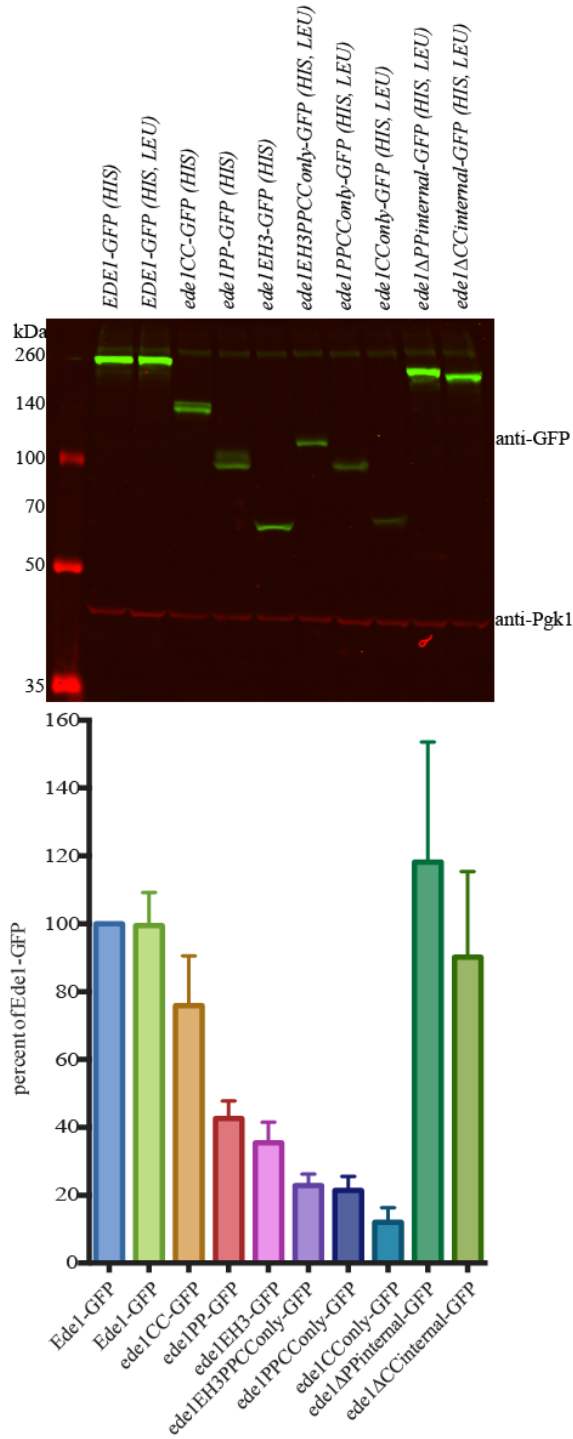


Figure 3.1 Localization of Ede1-GFP truncation mutants

(A) Schematic diagram of full-length Ede1 and the truncation constructs that were integrated at the *EDE1* locus. A C-terminal GFP tag, present on all constructs, is not shown. (B) Representative images from the first frame of movies of cells expressing the indicated GFP-tagged constructs imaged in the same field as Ede1-GFP reference cells, which have been labeled with FM4-64 (magenta). Movies of the GFP channel were taken at 2000 ms/frame for 4 min, immediately followed by a capture of a still image of FM4-64. Scale bar, 5 μ m. (C) Magnification of the inset of the yellow box outlined in B. (D and E) Circular kymographs of the mother (D) and bud (E) cortex from C. Time is along the x-axis and scale bars are 2 μ m and 20 seconds, as indicated.

A.



B.

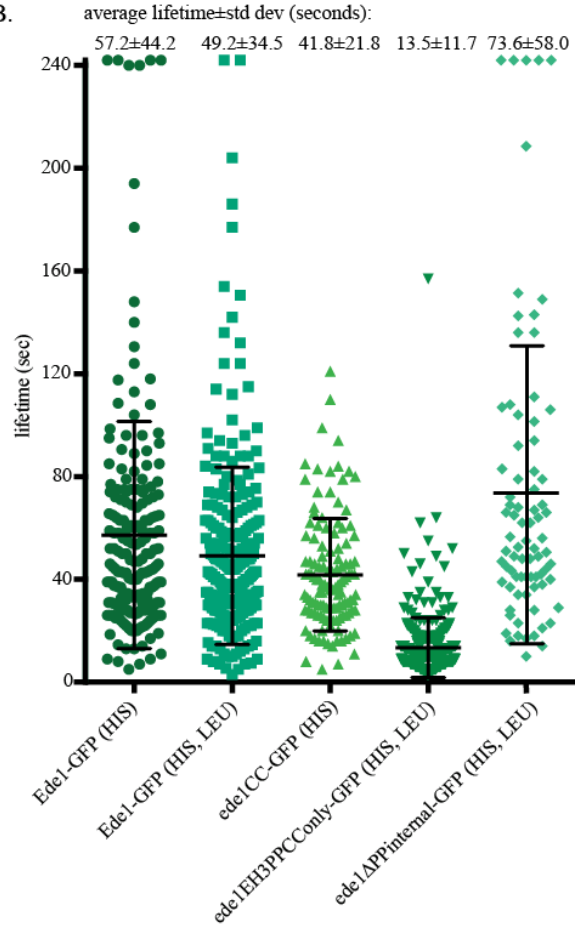


Figure 3.2 Ede1-GFP truncation protein expression and lifetimes

(A) Top: Western blot of whole cell lysates of cells of the indicated genotype. The blot was probed with rabbit anti-GFP (green) and mouse anti-Pgk1 (red, loading control) and exposed using an Odyssey imaging system (Licor). Bottom: Quantification of the intensity of GFP bands from the above western blot using the Odyssey imaging system. GFP bands were normalized to Pgk1 intensity and then expressed as a percentage of Ede1-GFP (*HIS*) intensity (first lane). Ede1-GFP (*LEU, HIS*) is a control that was generated in the same cloning method as other strains also marked with *HIS* and *LEU*. Error bars are +1 SD, n = four blots (B) Lifetimes of individual patches of the indicated Ede1-GFP truncation mutants were calculated from kymograph analysis of movies taken at 2000 ms/frame frame rate, for a total of four minutes. Patches that persisted through the duration of the movie were counted as 240 sec.

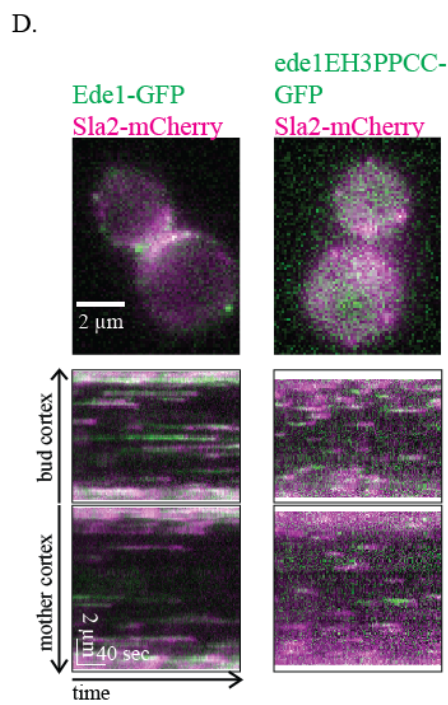
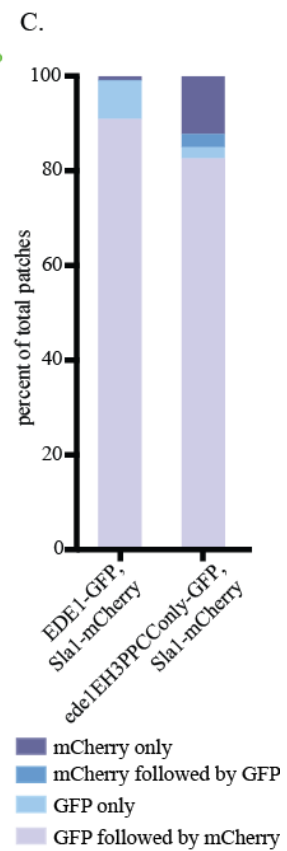
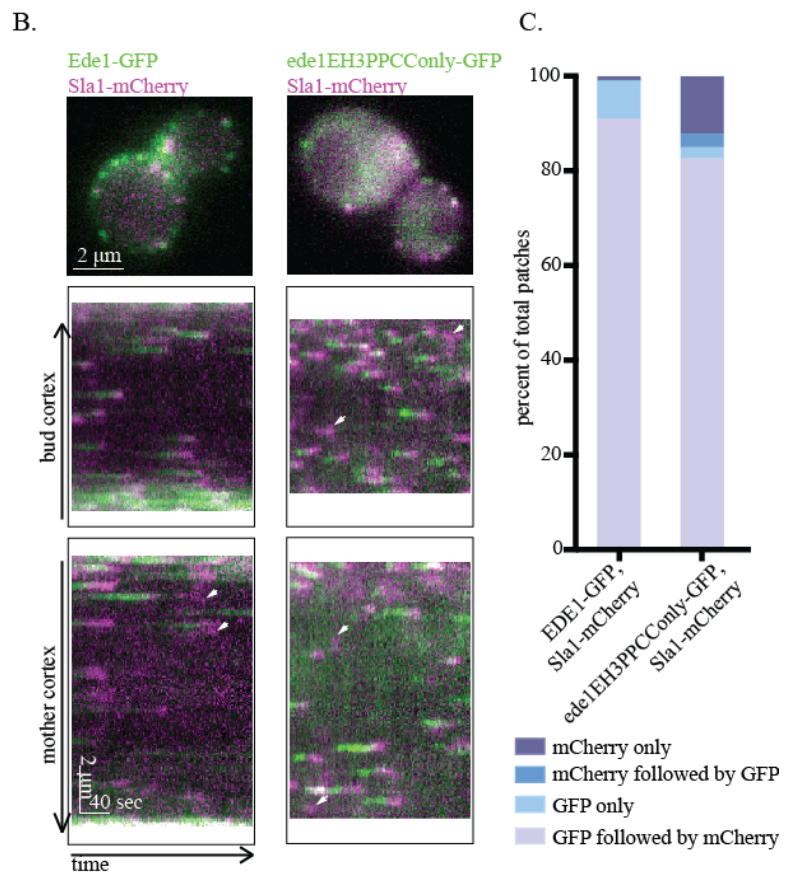
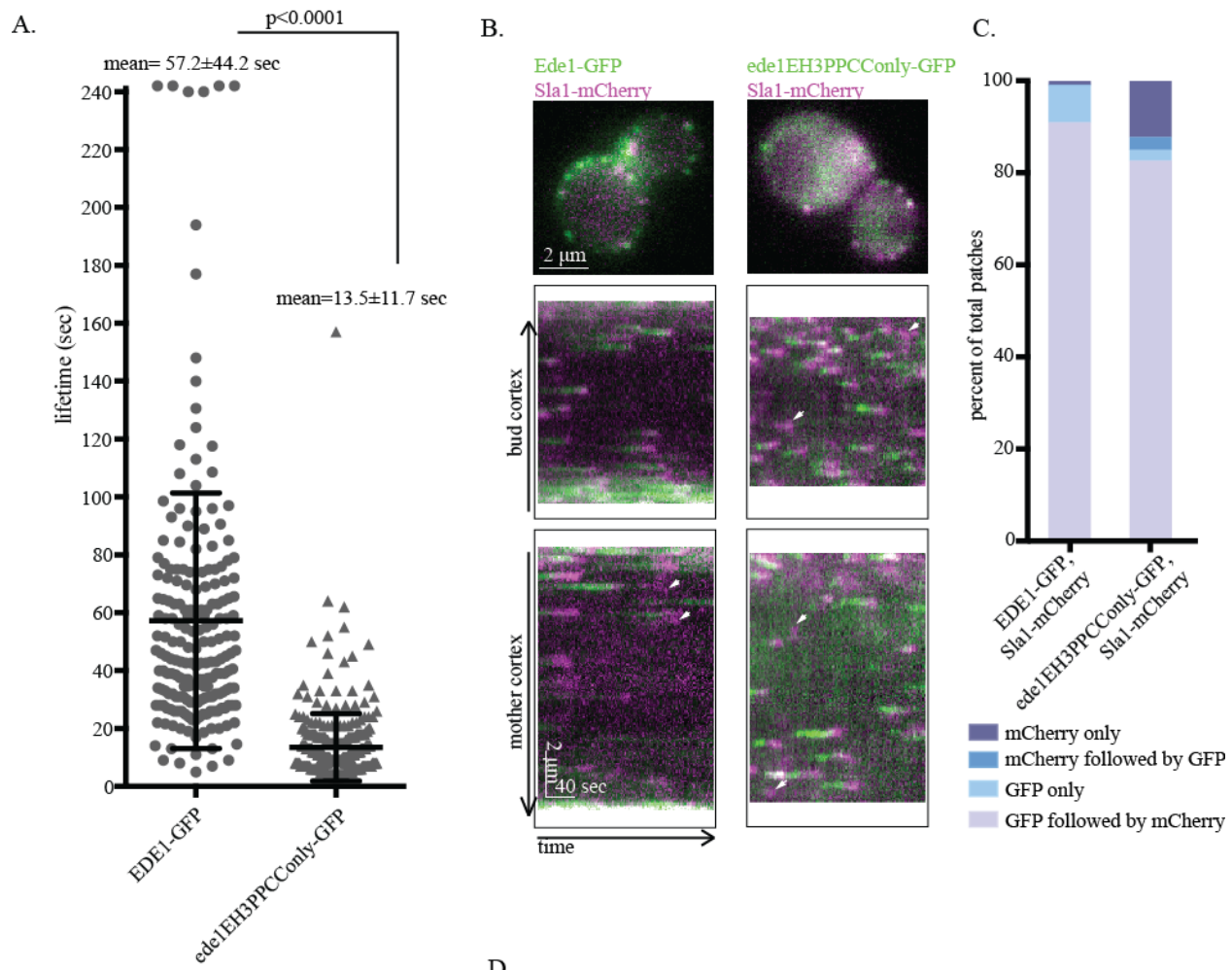


Figure 3.3 A construct containing the coiled-coil domain, third EH domain, and PxxP region is sufficient to recruit coat proteins.

(A) Lifetimes of individual Ede1 patches from Ede1-GFP vs. *ede1EH3PPCConly*-GFP expressing cells. Mean \pm standard deviation are shown. P-values were calculated using student's t-test. (B) Ede1-GFP variants were imaged with Sla1-mCherry for 4 minutes at 2 sec/frame using simultaneous dual-color imaging. The first frame of a movie of a representative cell is shown along with circular kymographs of the mother and bud cortex. White arrows indicate "Sla1-mCherry only patches". Scale bars, 2 μ m, 40 seconds. (C) The patch traces identified in kymographs were analyzed by eye and segregated into one of four categories depending on the relative arrival of GFP and mCherry: GFP or mCherry alone, or GFP followed by mCherry, or mCherry followed by GFP. The percentage of each category is shown (n= >465 patches/strain). (D) Ede1-GFP variants were imaged with Sla2-mCherry for 4 minutes at 2 sec/frame using simultaneous dual-color imaging. The first frame of a movie of a representative cell is shown along with circular kymographs of the mother and bud cortex. White arrows indicate "Sla1-mCherry only patches". Scale bars, 2 μ m, 40 seconds.

ede1EH3PPCC and ede1ΔCCinternal strains have normal numbers of sites, but altered maturation timing

As a readout of endocytic function, we examined the number of sites formed and the timing of coat maturation in cells expressing Ede1 truncations. Toward this end, we C-terminally tagged the *ede1EH3PPCC*only and *ede1ΔCCinternal* truncations of Ede1 with 13xmyc and used Sla1-GFP as a reporter for endocytosis, as it is highly sensitive to small perturbations in individual patch dynamics (Kaksonen et al., 2003) (Figure 3.4A), unlike FM4-64 or Lucifer Yellow uptake in bulk assays, which display insignificant or inconsistent phenotypes in *ede1Δ* cells (Reider et al., 2009; Stimpson et al., 2009). We chose to further study *ede1ΔCCinternal* in addition to *ede1EH3PPCC*only. Although the coiled-coil is necessary but not sufficient for efficient plasma membrane localization, and thus much of *ede1ΔCCinternal* is cytosolic, some of the protein is recruited to the plasma membrane, and we wanted to test whether this would provide any endocytic function.

Consistent with results from previous studies, we observed a significantly decreased number of endocytic sites in *ede1Δ* cells (Figure 3.4B, C). Surprisingly, we found that expression of just a portion of the full length protein, *EH3PPCC*only-myc, could facilitate formation of the normal number of Sla1-GFP initiations in a 90 second movie (Figure 3.4B, C). Even more surprisingly, we observed that, even though *ede1ΔCCinternal* is poorly recruited to the plasma membrane, as assessed by images of *ede1ΔCCinternal*-GFP, it can also facilitate formation of the normal number of Sla1-GFP initiations (Figure 3.1B-E). It is possible that patch initiation is rescued even though there is very little recruitment of *ede1ΔCCinternal* if later arriving coat proteins are recruited to these patches by the partially-localized truncation mutants. To test this possibility, we imaged *ede1ΔCCinternal*-GFP with Sla1-mCherry and found that 82.1% of *ede1ΔCCinternal*-GFP patches counted recruited Sla1-mCherry even though they displayed very faint GFP signals (Figure 3.4E). It is striking that two very different Ede1 truncation constructs can provide some endocytic function, suggesting that there might be redundancy in the endocytic site initiation mechanism. However, Sla1-GFP lifetimes were abnormal in strains expressing both constructs (Figure 3.4D), indicating that proper maturation timing is more sensitive to perturbations in Ede1.

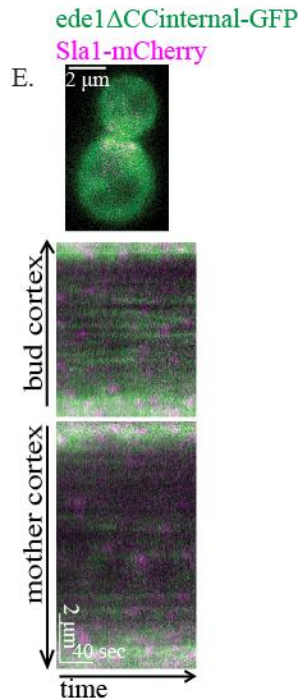
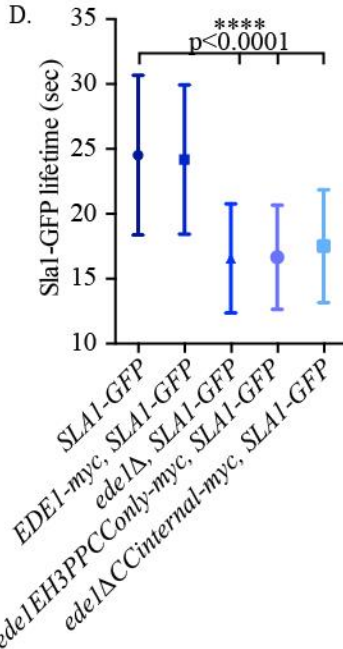
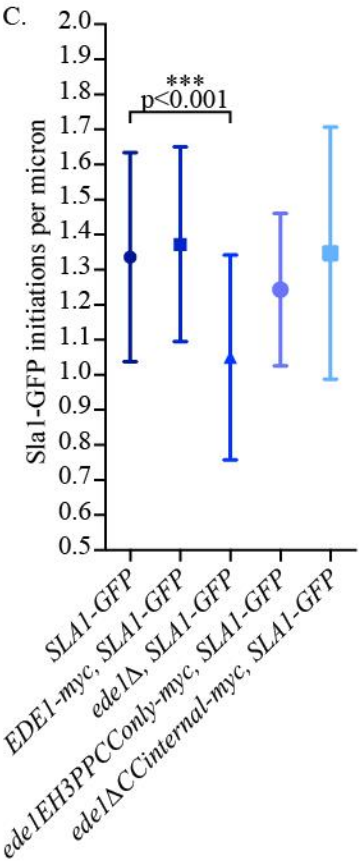
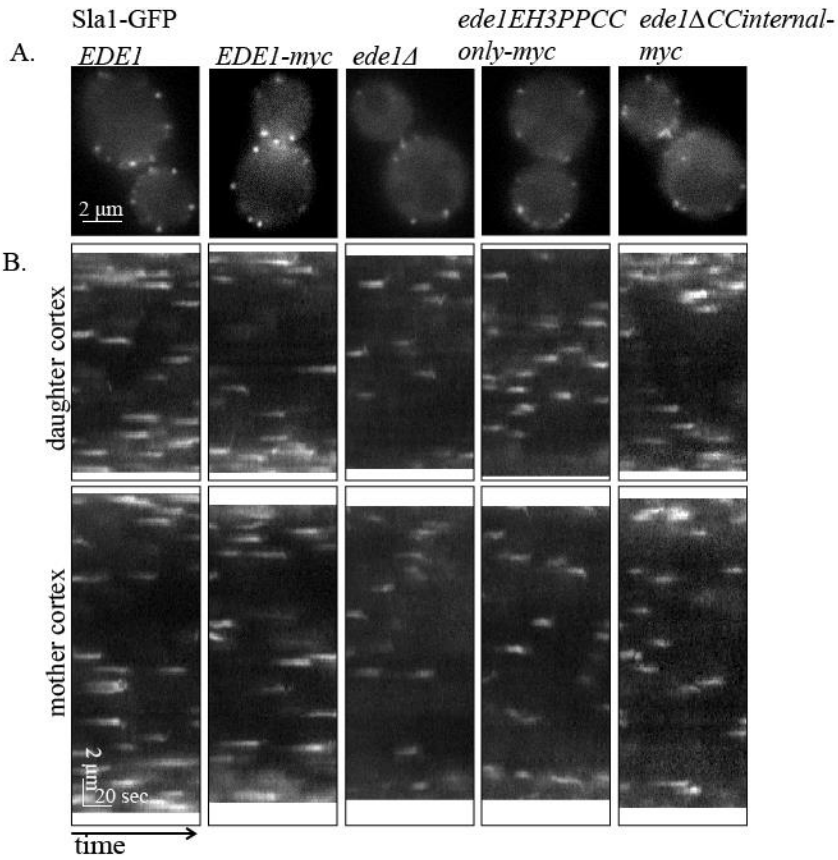


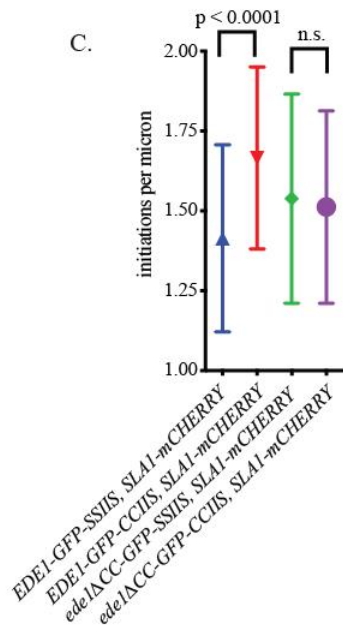
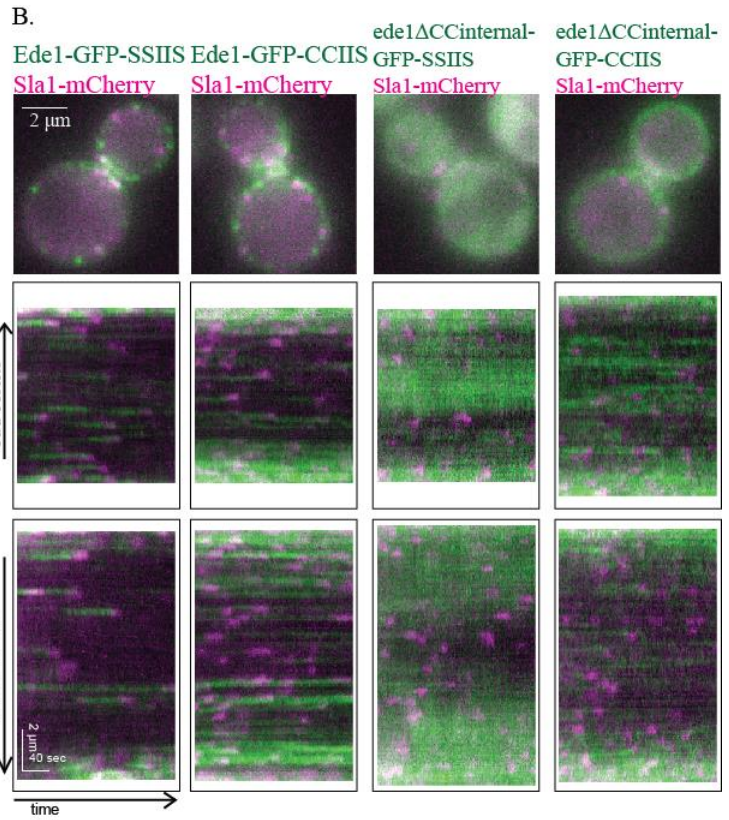
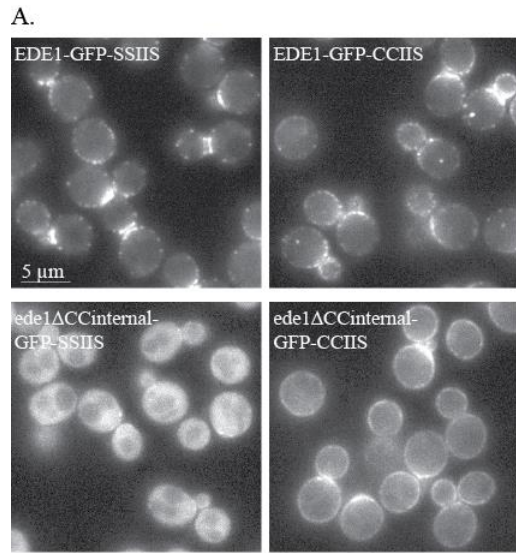
Figure 3.4 *ede1^{EH3PPCC}Only* and *ede1^{ΔCCinternal}* facilitate endocytic initiation, but not maturation timing

(A) 90-second movies of Sla1-GFP in cells expressing 13xmyc tagged Ede1 truncations were taken at 1 second/frame. The first frame from a representative movie of a single cell is shown. Scale bar, 5 μm . (B) Circular kymographs of the bud and mother cortex of the cells shown in A., scale bars 2 μm and 20 seconds. (C) Quantification of kymograph analysis of the number of patches that start or initiate during a 90 second movie ($n > 23$ cells/strain) in cells of the indicated genotype (see materials and methods). P-values calculated using student's t-test. (D) Quantification of the lifetime of Sla1-GFP ($n > 247$ patches) in cells of the indicated genotype. (E) *ede1^{ΔCCinternal}*-GFP and Sla1-mCherry were imaged for 4 minutes at 2 sec/frame with approximately 300 ms delay between channels. The first frame of a movie of a representative cell is shown, in addition to a circular kymograph of the bud and mother cortex. Scale bar 2 μm and 40 seconds

Ede1 coiled-coil domain functions to coalesce Ede1 molecules

Since loss of the Ede1 coiled-coil domain results in significantly reduced localization of the truncations to the plasma membrane, we tested whether artificially tethering *ede1* Δ CCinternal-GFP to the plasma membrane can restore normal Sla1 lifetimes. We accomplished this by appending the C-terminus with a CCaaX box from Ras2 (CCIIS), which is prenylated and palmitoylated, and directed mainly to the plasma membrane (Chen and Thorner, 2007). As a control, we also generated a strain in which the prenyl and palmitoyl acceptor cysteine sites have been mutated to serines (SSIIS). Compared to these non-prenylated, non-palmitoylated controls, CCIIS-tagged full length and *ede1* Δ CCinternal constructs were stably associated with the plasma membrane (Figure 3.5A). Full length Ede1-GFP-CCIIS formed stable punctae, while *ede1* Δ CCinternal-GFP-CCIIS was recruited uniformly around the cortex. Using kymograph analysis around the cell cortex, diffuse punctae of *ede1* Δ CCinternal-GFP-CCIIS could also be seen above the halo of plasma membrane fluorescence. Sla1-mCherry was specifically recruited to these diffuse punctae in *ede1* Δ CCinternal-GFP-CCIIS cells, and not to the halo of *ede1* Δ CCinternal-GFP-CCIIS fluorescence around the entire plasma membrane (Figure 3.5B). Interestingly, cells expressing Ede1-GFP-CCIIS initiated more sites compared to the SSIIS control, while cells expressing *ede1* Δ CCinternal-GFP-CCIIS initiated a similar number of sites compared to its SSIIS control (Figure 3.5C). We hypothesized that oligomerization by the coiled-coil domains is required for efficiently coalescing Ede1 into punctae at the plasma membrane.

To test oligomerization by the coiled-coils, we performed a co-immunoprecipitation experiment on diploids expressing Ede1-GFP and a 13xmyc tagged Ede1 construct. By precipitating Ede1-GFP as the bait protein and blotting against myc (9E10) for the presence of the Ede1 truncation construct, we found that in every case where the truncation contains the coiled-coils, including the coiled-coils alone (*ede1*CConly-myc), we were able to observe an interaction with Ede1-GFP (Figure 3.5D, lanes 1, 3-5). However, the *ede1* Δ CCinternal-myc truncation could not be precipitated with the full length Ede1-GFP bait (Figure 3.5D, lane 2). This is consistent with the conclusion that *ede1* Δ CCinternal-GFP-CCIIS plasma membrane localization is diffuse rather than in distinct punctae because the protein is unable to oligomerize. This adds to previous evidence suggesting that Ede1 oligomerization is a key step in site initiation.



D.

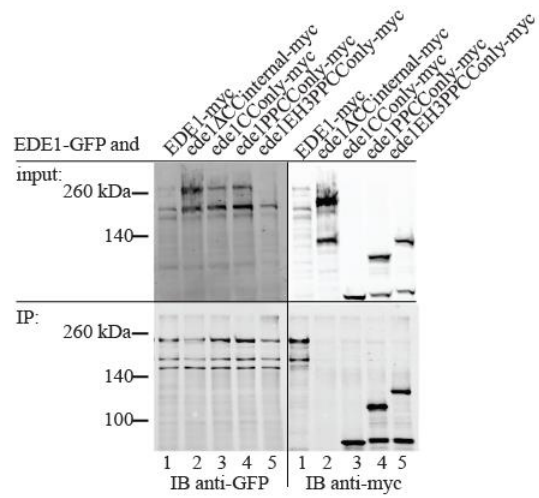


Figure 3.5 Coiled-coils contribute to endocytic site localization by aggregating Ede1 molecules

(A) Ede1-GFP or *ede1*⊗CCinternal-GFP were tagged with a prenylation motif (CCIIS) or a non-prenylated control (SSIIS) and expressed at the endogenous locus. Scale bar, 5 μm. (B) GFP constructs from (A) were expressed with Sla1-mCherry and imaged for 4 minutes at 2 sec/frame. Each channel was imaged separately at 500ms/exposure. The first frame of a movie of a representative cell is shown, followed by a circular kymograph of the bud and mother cortex. Scale bars, 2 μm and 40 seconds. (C) Quantification of kymograph analysis of the number of patches that start or initiate during a 90 second movie (n>65 cells/strain) in cells of the indicated genotype (see materials and methods). P-values calculated using student's t-test. (D) Whole cell lysates of diploid cells with the indicated genotype were subjected to immunoprecipitation using mouse anti-GFP antibody. The resulting immunoprecipitated proteins were subjected to SDS-PAGE and western blotting, using rabbit anti-GFP to detect the bait (Ede1-GFP) and mouse anti-myc (9E10) to detect the prey Ede1-13xmyc tagged constructs.

Human Eps15 can provide Ede1 functions in yeast

Human Eps15 is an important adapter protein in clathrin-mediated endocytosis. Like Ede1, it arrives to the endocytic site early in the endocytic pathway. Since Eps15 has a very similar domain structure to Ede1, containing central coiled-coils for dimerization, three EH domains, and ubiquitin interacting motifs, we tested whether full length Eps15 can function in the place of Ede1 in yeast. We first inserted the human *EPS15* cDNA, appended to a C-terminal GFP tag, into the *EDE1* locus, using the *EDE1* promoter to drive expression. Western blot analysis shows that expression of Eps15-GFP is approximately 20% that of Ede1-GFP (Figure 3.6A). However, even though it was expressed at a much lower level than Ede1, Eps15-GFP localized to endocytic sites at the plasma membrane (Figure 3.6B, C). In addition, Eps15-GFP appeared at the plasma membrane with similar timing to Ede1, arriving before Sla1. Approximately 78.3% of kymograph traces analyzed showed Eps15-GFP was followed by Sla1-mCherry at plasma membrane punctae, compared to 94.6% for Ede1-GFP.

Because Eps15 was expressed at such a low level from the *EDE1* promoter, we wanted to test whether increasing the expression to normal Ede1 levels would increase the frequency of coat (Sla1) recruitment. We increased expression by inserting the *EPS15* cDNA, tagged with GFP, under the *TEF1* (translation elongation factor EF1-alpha) promoter at the *URA3* locus. The *TEF1* promoter expresses proteins constitutively at a high level (Mumberg et al., 1995). Moving *EPS15* out of the *EDE1* locus also allowed us to express Eps15 in the presence or absence of Ede1, allowing us to test whether there was competition for recruitment to endocytic sites. Using the *TEF1* promoter increased Eps15 expression approximately 2-fold (Figure 3.6A,B). We also found that the presence of Ede1 prevented the majority of Eps15 from being recruited to the plasma membrane (Figure 3.6B). Furthermore, in this context, the vast majority of Sla1-mCherry patches on the plasma membrane were not preceded by the appearance of Eps15-GFP (Figure 3.6D, 16.9% of kymograph traces analyzed). When *EDE1* was deleted and Eps15-GFP was expressed from the *TEF1* promoter, Eps15-GFP formed more distinct patches than when Eps15-GFP was expressed from the *EDE1* promoter (Figure 3.6B,C Eps15-GFP (*EDE1pr*) *ede1*Δ vs. Eps15-GFP (*TEF1pr*) *ede1*Δ). However, the increased expression of Eps15 under the *TEF1* promoter did not significantly increase the frequency of patches in which Eps15-GFP precedes Sla1-mCherry (Figure 3.6D *EDE1p*-*EPS15*-GFP *ede1*Δ vs. *TEF1p*-*EPS15*-GFP *ede1*Δ, 78.3% vs. 82.0% of kymograph traces analyzed).

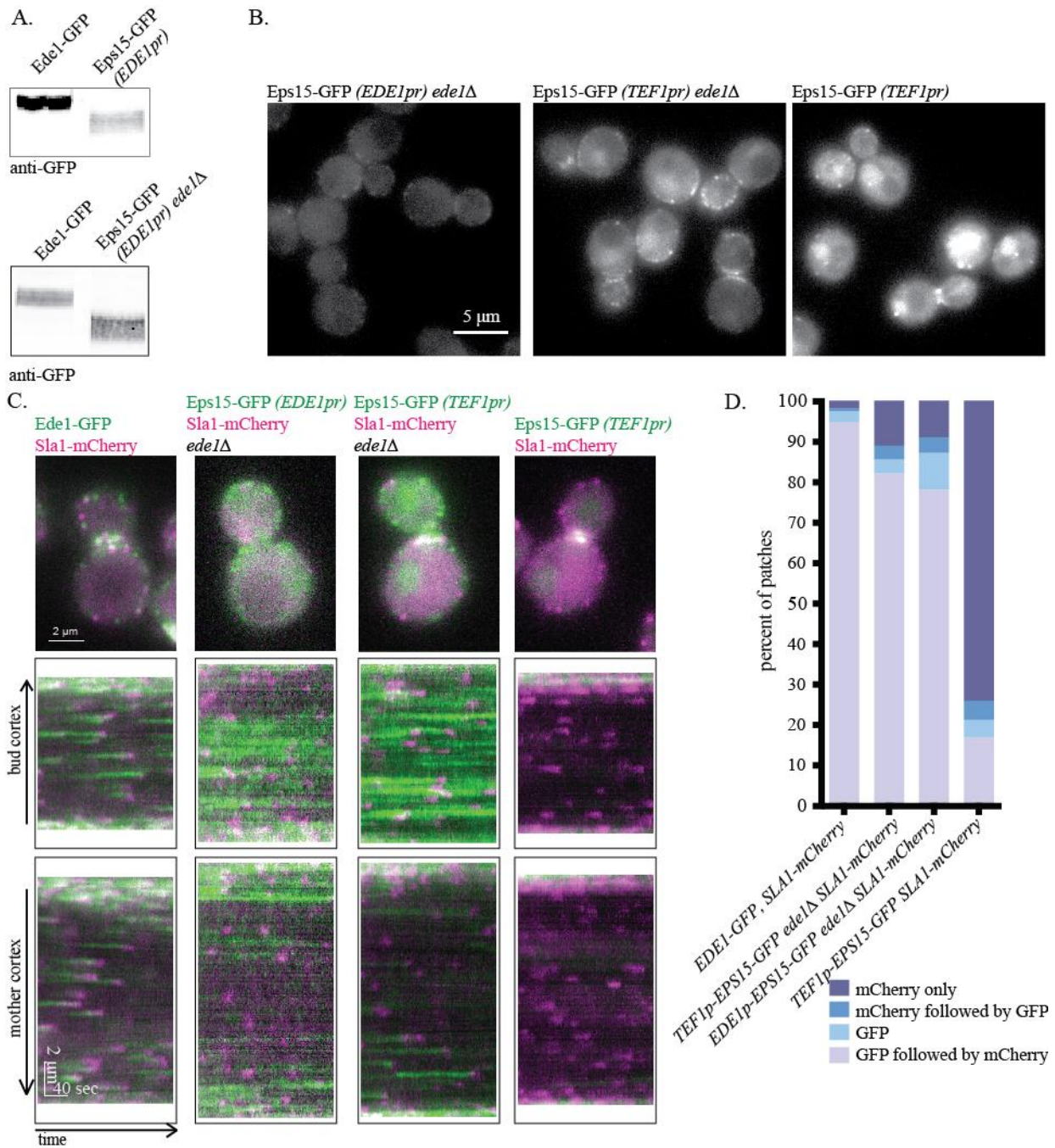


Figure 3.6 Eps15 can function as an endocytic site initiator in the absence of Ede1

(A) Western blot of whole cell lysates of cells expressing the indicated Eps15-GFP construct. Both the top and bottom blots were probed with rabbit anti-GFP. (B) Representative still images of cells expressing the indicated Eps15-GFP construct. (C) GFP constructs from (B) were expressed with Sla1-mCherry and imaged for 4 minutes at 2 sec/frame. Each channel was taken individually at 500ms/exposure. The first frame of a movie of a representative cell is shown, followed by a circular kymograph of the bud and mother cortex. Scale bars, 2 μm and 40 seconds. (D) The patch traces identified in kymographs from (C) were analyzed by eye and segregated into one of four categories depending on the relative arrival order for GFP and mCherry: GFP or mCherry alone, GFP followed by mCherry, or mCherry followed by GFP. The percentage of each category is shown (n>480 patches)

Discussion

Clathrin-mediated endocytosis is an essential process that is required for the internalization of certain receptors and materials from the plasma membrane or outside the cell. The regulation of endocytic site formation is a complex process, with many proteins known to play a role in ensuring proper formation and maturation of the site. Since CME site initiation is a crucial regulatory point, I chose to perform an in-depth study on the endocytic adapter/scaffolding protein, Ede1. My goal was to elucidate its role in determining site initiation in yeast. We analyzed the expression, localization, and function of an extensive array of Ede1 truncation constructs to understand each domain's role in both localization and function. By systematically teasing apart the behavior of each domain alone or in combinations, we hoped to identify specific protein-protein interactions that are necessary or sufficient for determining either site placement or the correct timing of site maturation.

We found that the minimal domains required for efficient endocytic site localization included the third EH domain, the proline-rich region, and the coiled-coil. A truncation mutant containing only these domains was able to recruit downstream endocytic proteins. However, lifetimes of this truncation in plasma membrane patches were much shorter, indicating that this truncation does not fully reconstitute all of Ede1's regulatory functions. One possible explanation for this finding is that one of the removed domains recruits cargo or another endocytic coat protein that in turn contributes to the characteristically longer and more variable lifetimes of endocytic events. Further work revealed that the coiled-coil domain is necessary for localization of Ede1 to plasma membrane punctae. Interestingly, artificial localization of *ede1* Δ CCinternal-GFP to the plasma membrane did not rescue wild-type localization. Instead, PM-targeted *ede1* Δ CCinternal-GFP was distributed uniformly around the cell cortex, indicating that the coiled-coil domain is required to coalesce individual Ede1 molecules into an initiating site. This is likely due to the oligomerization activity of the coiled-coils. Surprisingly, when expressed without artificial PM-targeting, lack of efficient localization of *ede1* Δ CCinternal-GFP to plasma membrane punctae did not greatly affect site initiation or placement since Sla1 could be recruited to faint and diffuse *ede1* Δ CCinternal-GFP patches. These results with two very different constructs composed of different domains are particularly surprising, as they illustrate the apparent internal redundancy of Ede1 in its function as an endocytic site initiator.

Finally, we found that the human protein Eps15 could function in place of Ede1 as an initiator of endocytic sites in yeast. Expression of Eps15 in yeast lacking Ede1 recapitulates the standard timing of endocytic events observed in strains expressing wild-type Ede1. Most importantly, Eps15 was also able to recruit downstream yeast coat proteins. In addition, Ede1 can compete with Eps15 when expressed in the same cell, indicating they both likely play the same role in endocytosis. Whether Eps15 is able to interact with the yeast homologues of its known binding partners in human cells will be interesting to test. It will be informative to determine which yeast proteins Eps15 interacts with, and if its interaction profile differs from the Ede1 interaction profile. To our knowledge, we are the first to express Eps15 in yeast and to identify it as a functional homolog of Ede1, which has important implications for our understanding of both proteins and how they function in CME in their respective systems.

Materials and methods

Yeast Strains and plasmids

Cells were maintained on rich media (YPD) at either 25°C or 30°C.

Strain	Genotype
DDY1102	<i>MATa/MATα, ade2-1/ADE2, his3Δ200/ his3Δ200, leu2-3,112/ leu2-3,112, ura3-52/ ura3-52, lys2-801/LYS2</i>
DDY904	<i>MATα, ade2-1, his3Δ200, leu2-3,112, ura3-52, lys2-801</i>
RLY17	<i>MATa, ede1PP-GFP(Δ593-1381)::HIS3, his3Δ200, leu2-3,112, ura3-52</i>
RLY56	<i>MATα, EDE1-GFP::HIS, his3Δ200, leu2-3,112, SLA1-mCherry::HIS, ura3-52</i>
RLY77	<i>MATa/MATα, ede1Δ::HIS3/EDE1, his3Δ200/ his3Δ200, leu2-3/leu2-3, lys2-801/LYS, ura3-52/ura3-52</i>
RLY86	<i>MATα, ede1Δ::ede1COnly(Δ6-586, Δ883-1376)-GFP::HIS3::LEU2, his3Δ200, leu2-3,112, lys2-801, ura3-52</i>
RLY88	<i>MATα, ede1Δ::ede1PPCOnly(Δ6-366, Δ883-1376)-GFP::HIS3::LEU2, his3Δ200, leu2-3,112, ura3-52</i>
RLY90	<i>MATα, ede1Δ::ede1Δ CCinternal(Δ593-882)-GFP::HIS3::LEU2, his3Δ200, leu2-3,112, LYS, ura3-52</i>
RLY99	<i>MATα, ede1Δ::EDE1-GFP::HIS3::LEU2, his3Δ200, leu2-3,112, LYS2, ura3-52</i>
RLY109	<i>MATa, ede1Δ::ede1Δ CCinternal(Δ593-882)-GFP::HIS3::LEU2, his3Δ200, leu2-3,112, SLA1-mCherry::HIS3, ura3-52</i>
RLY125	<i>MATa, ede1Δ::ede1Δ PPinternal(Δ366-592)-GFP::HIS3::LEU2, his3Δ200, leu2-3,112, lys2-801, ura3-52</i>
RLY133	<i>MATα, ede1Δ::ede1EH3PPCOnly(Δ6-231, Δ883-1376)-GFP::HIS3::LEU2, his3Δ200, leu2-3,112, LYS2, ura3-52</i>
RLY143	<i>MATa, ede1Δ::ede1EH3PPCCinternal(Δ6-231, Δ883-1376)::LEU2, EDE1-GFP::HIS3, his3Δ200, leu2-3,112, LYS, SLA1-mCherry::HIS3, ura3-52</i>
RLY153	<i>MATa, ede1Δ::ede1EH3PPCOnly(Δ6-231, Δ883-1376)-13xmyc::HIS3::LEU2, his3Δ200, leu2-3,112, SLA1-GFP::HIS3, ura3-52</i>
RLY155	<i>MATa, ede1Δ::ede1Δ CCinternal(Δ593-882)-13xmyc::HIS3::LEU2, his3Δ200, leu2-3,112, SLA1-GFP::HIS3, ura3-52</i>
RLY175	<i>MATα, ede1Δ::EDE1::LEU, EDE1-myc::HIS3, his3Δ200, leu2-3,112, SLA1-GFP::HIS3, ura3-52</i>
DDY3866	<i>MATa, EDE1-GFP::HIS3, his3Δ200, leu2-3,112, ura3-52</i>
DDY2734	<i>MATa, his3Δ200, leu2-3,112, lys2-801, SLA1-GFP::HIS3, ura3-52</i>
DDY3798	<i>MATa, ede1Δ::cgLEU2, his3Δ200, leu2-3,112, SLA1-GFP::KanMX6, ura3-52</i>

RLY235	<i>MATa, EDE1-GFP::HIS3::LEU2, his3Δ200, leu2-3,112, LYS, SLA2-mCherry::KAN, ura3-52</i>
RLY237	<i>MATa, ede1Δ::ede1EH3PPCOnly(Δ6-231, Δ883-1376)-GFP::HIS3::LEU2, his3Δ200, leu2-3,112, LYS, SLA2-mCherry::KAN, ura3-52</i>
RLY411	<i>MATa, ede1Δ::EDE1-GFP-CCIIS::LEU2, his3Δ200, leu2-3, 112, LYS, ura3-52</i>
RLY413	<i>MATa, ede1Δ::EDE1-GFP-SSIIS::LEU2, his3Δ200, leu2-3, 112, LYS, ura3-52</i>
RLY415	<i>MATa, ede1Δ::ede1ΔCCinternal(Δ562-883)-GFP-CCIIS::LEU2, his3Δ200, leu2-3, 112, LYS, ura3-52</i>
RLY417	<i>MATa, ede1Δ::ede1ΔCCinternal(Δ562-883)-GFP-SSIIS::LEU2, his3Δ200, leu2-3, 112, LYS, ura3-52</i>
RLY421	<i>MATα, ede1Δ::EDE1-GFP-SSIIS::LEU2, his3Δ200, leu2-3, 112, LYS, SLA1-mCherry::HIS, ura3-52</i>
RLY423	<i>MATα, ede1Δ::EDE1-GFP-CCIIS::LEU2, his3Δ200, leu2-3, 112, LYS, SLA1-mCherry::HIS, ura3-52</i>
RLY425	<i>MATa, ede1Δ::ede1ΔCCinternal(Δ562-883)-GFP-SSIIS::LEU2, his3Δ200, leu2-3, 112, LYS, SLA1-mCherry::HIS, ura3-52</i>
RLY427	<i>MATa, ede1Δ::ede1ΔCCinternal(Δ562-883)-GFP-CCIIS::LEU2, his3Δ200, leu2-3, 112, LYS, SLA1-mCherry::HIS, ura3-52</i>
RLY443	<i>MATa, ede1Δ::LEU2, his3Δ200, leu2-3,112, LYS2, SLA1-mCherry::HIS3, ura3-52</i>
RLY450	<i>MATa, ede1Δ::Eps15-GFP::LEU2, his3Δ200, leu2-3,112, LYS2, ura3-52</i>
RLY452	<i>MATa, ede1Δ::Eps15-GFP::LEU2, his3Δ200, leu2-3,112, LYS2, SLA1-mCherry::HIS3, ura3-5</i>
RLY457	<i>MATa, his3Δ200, leu2-3,112, LYS2, ura3-52::TEF1p-Eps15-GFP::URA3</i>
RLY459	<i>MATa, ede1Δ::HIS3, his3Δ200, leu2-3,112, LYS2, ura3-52::TEF1p-Eps15-GFP::URA3</i>
RLY465	<i>MATa, ede1Δ:HIS, his3Δ200, leu2-3,112, LYS2, SLA1-mCherry::HIS3, ura3-52::TEF1p-Eps15-GFP::URA3</i>
RLY471	<i>MATa, his3Δ200, leu2-3,112, LYS2, SLA1-mCherry::HIS3, ura3-52::TEF1p-Eps15-GFP::URA3</i>

EDE1 truncations were constructed either using a PCR-based C-terminal truncation method described in (Longtine et al., 1998) or by using pBluescript SK II containing the *EDE1* ORF with -385 bp upstream and +397 bp downstream from the genomic sequence. The downstream sequence is interrupted at +138 bp with the *LEU2* ORF with 646 bp of upstream sequence and 477 bp of downstream sequence from the genomic sequence, which was used as a selectable marker. Each truncation was then tagged with either 13xmyc or GFP using the C-terminal tagging method described in (Longtine et al., 1998).

EDE1 prenylation constructs were generated from the pBluescript SKII *EDE1* plasmid above by replacing the stop codon with GGSGGS+GFP (S65T) +QSGDQISEPGTLDASAPGGNTSEASKSGSGG+CCIIIS or GGSGGS+GFP (S65T) +QSGDQISEPGTLDASAPGGNTSEASKSGSGG+SSIIS.

EPS15 cDNA was cloned from Eps15-pmCherryN1 (Taylor et al., 2011) and cloned into the pBluescript SKII *EDE1* plasmid described above for *EDE1p-EPS15-GFP*. For *TEF1p-EPS15-GFP*, the same *EPS15* cDNA was cloned into pRS306 with 408 bp of the upstream region of the *TEF1* sequence. This was then integrated into the *URA3* locus.

Live Cell Imaging

Cells were grown to log phase at 25°C in imaging media (synthetic medium lacking tryptophan) and immobilized on concanavalin A-coated coverslips. All images except those in Figure 3.3 were obtained using a Nikon Eclipse Ti microscope equipped with a Plan Apo VC 100x 1.4 objective and a Neo sCMOS camera (Andor Technology). Images presented in Figure 3.3 were obtained using an Olympus IX81 microscope equipped with either a 100x NA 1.4 objective (3.3B) or a 60x NA 1.45 objective (3.3D) and an Orca-ER camera (Hamamatsu). Simultaneous two-color imaging for Figure 3.3 was performed on the Olympus IX81 using a 488 nm argon-ion laser (Melles Griot) and a mercury lamp filtered through a 575/20-nm filter. Exposure time and frequency of acquisition for time-lapse series are as indicated in figure legends.

Images were processed using ImageJ (NIH) as previously described to threshold background noise (Kaksonen et al., 2003). Circular kymographs were generated using the segmented line tool to draw a circle around the cortex of the mother and daughter of a budding cell. Number of initiations was calculated from these circular kymographs by counting the number of patches that started past the first frame (those that also ended past the last frame were also counted). Lifetimes were measured by generating multiple kymographs around the cell (separated by two degrees, for 180 kymographs total) that are perpendicular to the cortex, and then measuring the pixel distance from the start to the finish of a patch. GFP and mCherry correlation analysis was performed using the same type of kymograph analysis and manually notating each distinguishable patch as mCherry alone, GFP alone, mCherry followed by GFP, or GFP followed by mCherry.

Immunoblotting

Yeast total cell extracts were prepared from log-phase cells as previously described (Foianni et al., 1994). Total cell extracts were subjected to SDS-PAGE and immunoblot analysis using mouse rabbit anti-GFP (Torrey Pines) and mouse anti-Pgk1 (Invitrogen) antibodies.

Immunoprecipitation

Approximately 70 OD of yeast cells were collected and kept frozen at -80°C overnight. Pellets were then resuspended in cold lysis buffer (50 mM HEPES-KOH, pH7.6, 150 mM KCl, 1 mM EGTA, 0.1% NP-40, and 1x Protease inhibitor cocktail (Roche)) and lysed using a mini-bead beater (Biospec) by beating at top speed for 30 seconds in two intervals at 4°C. Lysates were collected and clarified by spinning at 13,000 rpm in a benchtop microcentrifuge for 10 min at 4°C. Protein G Sepharose beads (GE) were then added to the supernatant and incubated for 1 hour at 4°C to pre-clear the clarified lysate. Beads were then removed and GFP tagged proteins were immunoprecipitated by adding 4.8 µg of mouse anti-GFP (Roche) to the pre-cleared, clarified lysate and incubating at 4°C for 2 hours. Protein G Sepharose beads (GE) were then added and incubated for another hour at 4°C. Beads were then collected and washed in 10x bead volume with wash buffer (50 mM HEPES-KOH, pH7.6, 150 mM KCl, 1 mM EGTA, and 10% glycerol) four times. Proteins were then eluted off the beads by boiling in 2x Laemmli sample buffer.

References

- Bi, E. and Park, H.-O. (2012). Cell polarization and cytokinesis in budding yeast. *Genetics* 191, 347–87.
- Boeke, D., Trautmann, S., Meurer, M., Wachsmuth, M., Godlee, C., Knop, M. and Kaksonen, M. (2014). Quantification of cytosolic interactions identifies Ede1 oligomers as key organizers of endocytosis. *Mol Syst Biol* 10, 756.
- Brach, T., Godlee, C., Moeller-Hansen, I., Boeke, D. and Kaksonen, M. (2014). The initiation of clathrin-mediated endocytosis is mechanistically highly flexible. *Current Biology* 24, 548–54.
- Carroll, S. Y., Stimpson, H. E. M., Weinberg, J., Toret, C. P., Sun, Y. and Drubin, D. G. (2011). Analysis of yeast endocytic site formation and maturation through a regulatory transition point. *Mol Biol Cell* 23, 657–68.
- Carroll, S. Y., Stirling, P. C., Stimpson, H. E. M., Giesselmann, E., Schmitt, M. J. and Drubin, D. G. (2009). A yeast killer toxin screen provides insights into a/b toxin entry, trafficking, and killing mechanisms. *Dev Cell* 17, 552–60.
- Chen, R. E. and Thorner, J. (2007). Function and regulation in MAPK signaling pathways: lessons learned from the yeast *Saccharomyces cerevisiae*. *Biochim Biophys Acta* 1773, 1311–40.
- Confalonieri, S. and Di Fiore, P. P. (2002). The Eps15 homology (EH) domain. *FEBS Lett* 513, 24–9.
- Cupers, P., Haar, ter, E., Boll, W. and Kirchhausen, T. (1998). Parallel dimers and anti-parallel tetramers formed by epidermal growth factor receptor pathway substrate clone 15. *J Biol Chem* 272, 33430–4.
- Foiani, M., Marini, F., Gamba, D., Lucchini, G. and Plevani, P. (1994). The B subunit of the DNA polymerase alpha-primase complex in *Saccharomyces cerevisiae* executes an essential function at the initial stage of DNA replication. *Mol Cell Biol* 14, 923–33.
- Gagny, B., Wiederkehr, A., Dumoulin, P., Winsor, B., Riezman, H. and Haguenaer-Tsapis, R. (2000). A novel EH domain protein of *Saccharomyces cerevisiae*, Ede1p, involved in endocytosis. *J Cell Sci* 113 (Pt 18), 3309–19.
- Godlee, C. and Kaksonen, M. (2013). Review series: From uncertain beginnings: initiation mechanisms of clathrin-mediated endocytosis. *J Cell Biol* 203, 717–25.
- Goode, B. L., Eskin, J. A. and Wendland, B. (2015). Actin and endocytosis in budding yeast. *Genetics* 199, 315–58.
- Kaksonen, M., Sun, Y. and Drubin, D. G. (2003). A pathway for association of receptors, adaptors, and actin during endocytic internalization. *Cell* 115, 475–87.
- Kaksonen, M., Toret, C. P. and Drubin, D. G. (2005). A modular design for the clathrin- and actin-mediated endocytosis machinery. *Cell* 123, 305–20.

- Longtine, M. S., McKenzie, A., Demarini, D. J., Shah, N. G., Wach, A., Brachat, A., Philippsen, P. and Pringle, J. R. (1998). Additional modules for versatile and economical PCR-based gene deletion and modification in *Saccharomyces cerevisiae*. *Yeast* 14, 953–61.
- Maldonado-Báez, L., Dores, M. R., Perkins, E. M., Drivas, T. G., Hicke, L. and Wendland, B. (2008). Interaction between Epsin/Yap180 adaptors and the scaffolds Ede1/Pan1 is required for endocytosis. *Mol Biol Cell* 19, 2936–48.
- Miliaras, N. B. and Wendland, B. (2004). EH proteins: multivalent regulators of endocytosis (and other pathways). *Cell Biochem Biophys* 41, 295–318.
- Mumberg, D., Müller, R. and Funk, M. (1995). Yeast vectors for the controlled expression of heterologous proteins in different genetic backgrounds. *Gene* 156, 119–22.
- Newpher, T. M., Smith, R. P., Lemmon, V. and Lemmon, S. K. (2005). In vivo dynamics of clathrin and its adaptor-dependent recruitment to the actin-based endocytic machinery in yeast. *Dev Cell* 9, 87–98.
- Peng, Y., Grassart, A., Lu, R., Wong, C. C. L., Yates, J., Barnes, G. and Drubin, D. G. (2015). Casein kinase 1 promotes initiation of clathrin-mediated endocytosis. *Dev Cell* 32, 231–40.
- Reider, A., Barker, S. L., Mishra, S. K., Im, Y. J., Maldonado-Báez, L., Hurley, J. H., Traub, L. M. and Wendland, B. (2009). Syp1 is a conserved endocytic adaptor that contains domains involved in cargo selection and membrane tubulation. *EMBO J* 28, 3103–16.
- Sieczkarski, S. B. and Whittaker, G. R. (2002). Dissecting virus entry via endocytosis. *J Gen Virol* 83, 1535–45.
- Stimpson, H. E. M., Toret, C. P., Cheng, A. T., Pauly, B. S. and Drubin, D. G. (2009). Early-arriving Syp1p and Ede1p function in endocytic site placement and formation in budding yeast. *Mol Biol Cell* 20, 4640–51.
- Taylor, M. J., Perrais, D. and Merrifield, C. J. (2011). A high precision survey of the molecular dynamics of mammalian clathrin-mediated endocytosis. *PLoS Biol* 9, e1000604.
- Tebar, F., Confalonieri, S., Carter, R. E., Di Fiore, P. P. and Sorkin, A. (1997). Eps15 is constitutively oligomerized due to homophilic interaction of its coiled-coil region. *J Biol Chem* 272, 15413–8.
- Tebar, F., Sorkina, T., Sorkin, A., Ericsson, M. and Kirchhausen, T. (1996). Eps15 is a component of clathrin-coated pits and vesicles and is located at the rim of coated pits. *J Biol Chem* 271, 28727–30.
- Weinberg, J. and Drubin, D. G. (2011). Clathrin-mediated endocytosis in budding yeast. *Trends Cell Biol* 22, 1–13.
- Wendland, B., McCaffery, J. M., Xiao, Q. and Emr, S. D. (1996). A novel fluorescence-activated cell sorter-based screen for yeast endocytosis mutants identifies a yeast homologue of mammalian eps15. *J Cell Biol* 135, 1485–500.

Chapter 4: Future directions

Further studies to dissect Ede1 function

This goal of my thesis work was to elucidate the regulation of endocytic site initiation through the scaffolding protein, Ede1, in the budding yeast *S. cerevisiae*. While Ede1 exerts a strong influence on CME initiation, mutants defective in this protein have very mild fluid-phase uptake and growth defects (Stimpson et al., 2009). It is possible that this very mild phenotype is a result of compensation by the endocytic machinery. To test whether this is true, and to better understand more about Ede1 function in general, one could use the auxin-mediated degron system (Eng et al., 2014; Nishimura et al., 2009) to rapidly degrade the Ede1 protein within minutes and observe how coat and actin proteins respond to immediate Ede1 depletion. If Ede1 acts as a nucleator of endocytic sites to scaffold many weak interactions, we may see a very dramatic reduction in endocytic site formation that recovers over time as the machinery can still interact, but much more slowly. If Ede1 is important for positioning sites, and therefore maintaining the polarization of the number of sites between the mother and bud, we may see that sites immediately depolarize after depletion. If we see no change, this indicates that Ede1 is not the only key protein for site initiation, and there may be a parallel pathway that works in conjunction with Ede1.

During the course of my thesis work, I generated many Ede1 truncations (Chapter 3) that can be used for further studies. For example, an informative experiment would be to artificially localize all of the truncations to the plasma membrane to see what downstream proteins are able to be recruited by the truncated versions of Ede1. An analogous experiment to complement this would be an affinity approach (Michelot et al., 2010) using purified Ede1 truncation constructs on 2-5 μm sized beads that could be incubated in yeast extract containing fluorescently tagged endocytic proteins. Time-lapse imaging of these beads could identify which proteins are recruited and whether the kinetics of recruitment is perturbed. These beads could additionally be used for mass-spectrometry to identify interacting proteins. Different truncation mutants would be expected to have different interaction profiles.

One particularly interesting truncation mentioned in Chapter 3 is the *ede1EH3PPC*Only truncation, which has a much shorter lifetime at endocytic sites compared to full-length Ede1. Despite its smaller size, it still recruits downstream coat proteins. One possibility is that this construct has bypassed some sort of checkpoint that would normally pause site maturation at the early and early coat protein stages (Chapter 1, Figure 1.1). An interesting hypothesis that has been proposed (Loerke et al., 2009) is that a checkpoint monitors the absence of cargo and halts endocytic site progression until cargo arrives. Further work investigating why endocytosis in cells expressing the *ede1EH3PPC*Only construct have accelerated endocytosis may provide insights into this possibility. It would be interesting to test for interactions made by full length Ede1 vs. *ede1EH3PPC*Only because proteins that interact with the full length, but not *ede1EH3PPC*Only would be candidate components of the checkpoint machinery. Another

experiment to test this cargo checkpoint hypothesis would be to do a genetic screen for mutants in other genes to see if any can be identified that accelerate endocytosis.

We also characterized a very specific interaction with the casein kinase Hrr25. It would be very interesting to test whether Ede1 phosphorylation by Hrr25 generates cross-talk between CME and other cellular processes that are also influenced by Hrr25, especially other trafficking pathways such as golgi trafficking (Lord et al., 2011) and autophagy (Tanaka et al., 2014). In addition, it was previously suggested that ubiquitination of Ede1 affects its ability to initiate endocytic sites (Weinberg and Drubin, 2014). Future work should address whether there is cross-talk between phosphorylation by Hrr25, or any other kinase, and ubiquitination. It was also shown from mass spectrometry of *in vitro* phosphorylated Ede1 that phosphorylation by Hrr25 is concentrated in the C-terminus between the coiled-coils and the UBA domain (Peng et al., 2015). A mutant of Ede1 in which 22 of these phosphorylated residues are mutated to either unphosphorylatable alanines (ede1-22A) or phosphomimetic aspartic acids (ede1-22D) fails to recruit Hrr25 (Peng et al., 2015). How these phosphorylations affect Hrr25 recruitment and the overall mechanism for Hrr25 recruitment or stabilization by Ede1 is still an open question.

Future studies to dissect Eps15 function in mammalian cells

One very important and interesting finding was that the human Eps15 could functionally replace Ede1 as an endocytic site initiator in yeast. This result indicates that there must be conserved features of these two proteins in CME, specifically in site initiation. Future work should test whether Eps15 functions in human cells in a manner similar to Ede1 in yeast. Previous work indicated that Eps15 interacts with the main clathrin adapter complex, AP-2 (Benmerah et al., 1996). Immunoelectron microscopy also suggested that, like Ede1, Eps15 stays at the rim of growing clathrin-coated pits, and therefore may function to coordinate AP-2 and clathrin recruitment to endocytic sites (Cupers et al., 1998). With recent advances in genome editing, it would now be possible to tag Eps15 with a fluorescent protein and image the spatiotemporal localization of endogenous Eps15. It is also now possible to genomically delete human *EPS15* and observe the behavior of other endocytic proteins such as clathrin and dynamin, or AP-2 and dynamin. In addition to deleting *EPS15*, the auxin-degron system, mentioned above, could also be used in mammalian cells to test the effects of acute Eps15 depletion.

Perspectives on clathrin-mediated endocytosis site initiation

The overarching goal of this thesis was to gain better insight into the mechanism of endocytic site initiation. Many different initiation mechanisms have recently been proposed: 1. stochastic interaction of AP-2 and clathrin at the plasma membrane (Cocucci et al., 2012), 2. initiation by the F-BAR proteins FCHo1/2, involving membrane bending activity and

recruitment of Eps15 and Intersectin (Henne et al., 2010), and 3. assembly of adapters at the plasma membrane through cargo clustering (Liu et al., 2010). It is possible that aspects of all three models are true and that there are redundant mechanisms for site initiation. A more general model that encompasses these three models is that weak, but cooperative, multivalent interactions among adapters and other early arriving proteins promote the nucleation of the endocytic site by a mechanism similar to a phase transition (Banjade and Rosen, 2014). To further analyze these protein-protein interactions in cells, future studies should use high precision microscopy to count how many of each type of molecule is present at endocytic sites as they are initiated and matured. These numbers would also be invaluable for mathematical modeling, which would also provide testable hypotheses for how endocytosis is initiated in cells.

Conclusions

Clathrin-mediated endocytosis (CME) is a very robust process that has a very predictable assembly and disassembly timeline. Much work has been put into elucidating the timing and functions of the individual proteins. However, to understand how CME functions and why it is so robust and predictable requires a deeper understanding of how the endocytic machinery is regulated and how each component interacts with the others. How is each step (site initiation, cargo capture, coat assembly, membrane bending, invagination, scission, etc.) regulated? What are the minimal components and key activities that are required for each step? How do protein-protein or protein-lipid interactions influence biophysical properties of endocytic sites, and how do they change as the site matures? Answering these questions will provide a basis for understanding how yeast CME progresses. In this study, I have dissected the functions of a key protein, Ede1, to elucidate more information about endocytic site initiation. The findings are expected to apply in other organisms owing to the high conservation of the endocytic machinery.

References

- Banjade, S. and Rosen, M. K. (2014). Phase transitions of multivalent proteins can promote clustering of membrane receptors. *Elife* 3.
- Benmerah, A., Bégue, B., Dautry-Varsat, A. and Cerf-Bensussan, N. (1996). The ear of alpha-adaptin interacts with the COOH-terminal domain of the Eps 15 protein. *J Biol Chem* 271, 12111–6.
- Cocucci, E., Aguet, F., Boulant, S. and Kirchhausen, T. (2012). The first five seconds in the life of a clathrin-coated pit. *Cell* 150, 495–507.
- Cupers, P., Haar, ter, E., Boll, W. and Kirchhausen, T. (1998). Parallel dimers and anti-parallel tetramers formed by epidermal growth factor receptor pathway substrate clone 15. *J Biol Chem* 272, 33430–4.
- Eng, T., Guacci, V. and Koshland, D. (2014). ROCC, a conserved region in cohesin's Mcd1 subunit, is essential for the proper regulation of the maintenance of cohesion and establishment of condensation. *Mol Biol Cell* 25, 2351–64.
- Henne, W. M., Boucrot, E., Meinecke, M., Evergren, E., Vallis, Y., Mittal, R. and McMahon, H. T. (2010). FCHo proteins are nucleators of clathrin-mediated endocytosis. *Science* 328, 1281–4.
- Liu, A. P., Aguet, F., Danuser, G. and Schmid, S. L. (2010). Local clustering of transferrin receptors promotes clathrin-coated pit initiation. *J Cell Biol* 191, 1381–93.
- Loerke, D., Mettlen, M., Yasar, D., Jaqaman, K., Jaqaman, H., Danuser, G. and Schmid, S. L. (2009). Cargo and dynamin regulate clathrin-coated pit maturation. *PLoS Biol* 7, e57.
- Lord, C., Bhandari, D., Menon, S., Ghassemian, M., Nycz, D., Hay, J., Ghosh, P. and Ferro-Novick, S. (2011). Sequential interactions with Sec23 control the direction of vesicle traffic. *Nature* 473, 181–6.
- Michelot, A., Costanzo, M., Sarkeshik, A., Boone, C., Yates, J. R. and Drubin, D. G. (2010). Reconstitution and protein composition analysis of endocytic actin patches. *Current Biology* 20, 1890–9.
- Nishimura, K., Fukagawa, T., Takisawa, H., Kakimoto, T. and Kanemaki, M. (2009). An auxin-based degron system for the rapid depletion of proteins in nonplant cells. *Nat Methods* 6, 917–22.
- Stimpson, H. E. M., Toret, C. P., Cheng, A. T., Pauly, B. S. and Drubin, D. G. (2009). Early-arriving Syp1p and Ede1p function in endocytic site placement and formation in budding yeast. *Mol Biol Cell* 20, 4640–51.

Tanaka, C., Tan, L.-J., Mochida, K., Kirisako, H., Koizumi, M., Asai, E., Sakoh-Nakatogawa, M., Ohsumi, Y. and Nakatogawa, H. (2014). Hrr25 triggers selective autophagy-related pathways by phosphorylating receptor proteins. *J Cell Biol* **207**, 91–105.

Weinberg, J. S. and Drubin, D. G. (2014). Regulation of clathrin-mediated endocytosis by dynamic ubiquitination and deubiquitination. *Current Biology*.